expressed as the dilution causing 50% plaque reduction: the neutralization titers of anti-HSV-1 mouse antiserum and anti-HSV-1 guinea pig antiserum were 1000 and 1600, respectively.

*Viral replication assay*

MCs or HOmMCs were plated on 35-mm dishes at a density of $3.7 \times 10^5$ cells per dish in 2 ml of the growth medium under standard conditions overnight. Cells were then infected with HF10 or Hh101 at multiplicities of infection (MOI) ranging between 0.03 and 3. To measure virus replication, cells were scraped from dishes at the indicated times, lysed by freeze–thaw and centrifuged at 3000 r.p.m. for 5 min. Viral titers were determined from the sample supernatants by plaque assay.

In vitro *delivery of HSV using MCs as carriers*

MCs were infected with Hh101 (MOI, 3) for 1 h at 37 °C; free virus was then removed and the cells were washed with phosphate-buffered saline (PBS) three times and resuspended in fresh medium. At 2 h after infection, the infected cells were trypsinized. The suspension was centrifuged at 1300 r.p.m. for 5 min at 4 °C. The collected cells were used as infected carrier cells.

SKOV3 cells were plated on 35-mm dishes at a density of $5.6 \times 10^5$ cells per dish in 2 ml of the growth medium. After 24 h, Hh101- ($3 \times 10^5$ PFU) or Hh101-infected carrier cells ($1 \times 10^5$ cells, MOI, 3) were added to the media, and we observed any resulting cytopathogenic effects (CPEs). At 24 h after infection, viral titers were determined from the sample supernatants by plaque assay.

In vitro *effects of anti-HSV-1 antiserum on HF-GFP*

HOmMCs were infected with HF-GFP (MOI, 3) for 1 h at 37 °C; free virus was then removed and the cells were washed with PBS three times and resuspended in fresh medium. At 2 h after infection, the infected cells were trypsinized. The suspension was then centrifuged at 1300 r.p.m. for 5 min at 4 °C. The collected cells were used as infected carrier cells.

SKOV3 cells were plated on 35-mm dishes. After 24 h, HF-GFP ($10^5$ PFU per dish) or HF-GFP-infected carrier cells ($10^4$ cells per dish) were added to the media with or without anti-HSV-1 mouse antiserum. At 24 h after infection, SKOV3 cells were photographed using the Leica (Wetglar, Germany) M205FA fluorescence stereomicroscope with a standard GFP filter set. At 30 h, SKOV3 cells were fixed with 4% formaldehyde and stained with 0.2% crystal violet solution. The number of plaques was counted under microscopy. The graphs (Figure 5e) were obtained from two independent experiments.

*Animal studies*

Animal studies were performed in accordance with guidelines issued by the Animal Center at Nagoya University School of Medicine. Female Balb/c slc nu/nu mice (5 to 6 weeks old) were purchased from Japan SLC (Hamamatsu, Japan). For surgical procedures, mice were anesthetized with an intraperitoneal injection of 7.2% chloral hydrate in sterile PBS (0.005 ml $g^{-1}$ body weight).

*Subcutaneous tumor model*

To determine the therapeutic efficacy of HF10, we used a subcutaneous (s.c.) tumor model. SKOV3 cells were cultured and passaged twice *in vitro*, and $5 \times 10^6$ cells were injected s.c. into the flanks of 5-week-old nude mice. At 8 days after tumor challenge, when s.c. tumors were ~10–15 mm in diameter, mice were treated with intratumoral (i.t.) injection of HF10 ($1 \times 10^7$ PFU). Animals in the first group were injected on days 8, 10 and 12. Animals in the second group were injected on days 8, 10, 12, 18, 20 and 22. Control mice were treated with i.t. injection of 1 ml PBS. Tumor volume was monitored for the indicated number of days after treatment.

*Intraperitoneal tumor model*

We confirmed that intraperitoneal (i.p.) injection of SKOV3 cells into 6-week-old female Balb/c nude mice resulted in peritoneally disseminated tumors, ascites, cachexia and death. To assess the efficacy of Hh101, this murine xenograft model was used. Nude mice ($n = 27$) were engrafted i.p. with $2 \times 10^6$ SKOV3 cells. HOmMCs were infected for 2 h with MOI = 3 of Hh101 and were used as carriers. After freezing and thawing at 2 h after infection, ~$5 \times 10^4$ PFU of Hh101 were detected as infectious viruses. To estimate the effect of Hh101 in minimally spread ovarian cancer, HOmMCs ($3 \times 10^6$ cells) infected with Hh101 were injected i.p. on days 3, 6 and 9. The control groups received 1 ml PBS or Hh101 ($5 \times 10^4$ PFU $ml^{-1}$) by i.p. injection on the same days. Mice of each group were followed up to record survival times.

To evaluate the role of Hh101 in more advanced disease, SKOV3 tumors were allowed to grow for 6 days before they were treated. Female Balb/c nude mice (6 weeks old )($n = 10$) were engrafted i.p. with $2 \times 10^6$ SKOV3 cells, and this animal group was treated with repeated injection on days 6, 9, 12, 15 and 18. Animals were followed up daily to record survival times.

*Localization of virus-associated GFP expression in mice with disseminated ovarian cancer*

Female Balb/c nu/nu mice (6 weeks old) were engrafted i.p. with $2 \times 10^6$ SKOV3 cells. On day 30, mice were randomized into two cohorts (control, HF-GFP treatment group). The control group received i.p. administration of 1 ml PBS. The HF-GFP treatment group was given $10^7$ PFU of HF-GFP i.p. After 24 h, mice were killed and tumors were examined using the Leica M205FA automated fluorescence stereomicroscope with a standard GFP filter set.

To assess the effect of anti-HSV-1 antiserum by using infected carrier cell, we injected control serum or anti-HSV-1 guinea pig antiserum of (500 µl per each mouse, × 1/100 dilution) i.p. into each mouse at 1 h before treatment. HOmMCs were preinfected with HF-GFP (MOI, 3) for 2 h and were washed in PBS. For this experiment, a disseminated ovarian cancer model ($1 \times 10^7$ SKOV3 cells, i.p.) was established in 6-week-old female Balb/c nu/nu mice. On day 14, mice were randomized qinto control, HF-GFP and HF-GFP-infected HOmMCs groups. The HOmMCs group was treated with $10^7$ cells of

HOmMC-infected HF-GFP. Mice were killed after 24 h and the intra-abdominal images were obtained by the fluorescence stereomicroscope. For each experiment, images were captured under identical exposure settings. Overlays were generated using Adobe Photoshop CS software (Adobe Systems, San Jose, CA).

### *Statistical methods*

Data were analyzed using the StatView statistical software package (SAS Institution, Cary, NC). The survival data were analyzed using the Kaplan–Meier method and the log-rank test. Differences in tumor volumes between the treated and control groups were analyzed by the Student's *t*-test. *P*-values $<0.05$ were considered statistically significant.

## Results

### *Intratumoral Administration of HSV mutants suppresses s.c. tumor growth of human ovarian cancer cells in nude mice*

We examined the ability of HF10 to control tumor cell growth in an *in vivo* model. We used an s.c. tumor model, because HF10 is fatal to immunodeficient animals when it is administered intravenously or intraperitoneally. The flanks of Balb/c-nu mice were s.c. injected with $5 \times 10^6$ SKOV3 cells. When tumors were palpable (day 8), i.t. injections of PBS or HF10 ($1 \times 10^7$ PFU) were made on days 8, 10 and 12 for group one, and on days 8, 10, 12, 18, 20 and 22 for group two. Injections (i.t.) with HF10 significantly reduced tumor growth compared with PBS-injected control animals (Figure 2a). Moreover, in group two, complete disappearance of tumors was observed in some animals (Figure 2b). Representative pictures of control and HF10-injected mice are shown (Figure 2c).

### In vitro *replication of HSV mutants in MCs, immortalized HOmMCs and SKOV3 cells*

To determine which cell line might be adequate for use as a carrier, we next tested the ability of HF10 and Hh101 to replicate in MCs, immortalized human omentum MCs and in SKOV3 cells. Human MCs may pose considerable advantages as vehicles for oncolytic virotherapy for ovarian cancer. First, MCs can be isolated from patients and grown in culture relatively easily. In addition, if isolated from the same patient that will be treated, autologous transplantation overcomes the difficulties related to immune rejection of the transplanted cells. Cells were infected at MOIs of 3 or 0.03. At MOI of 3, virus titers were ~10-fold higher in HOmMCs than in MCs or SKOV3 cells at 24 h after infection (Figures 3e, f). This correlated with the observation of more extensive and rapid CPEs in HOmMCs than SKOV3 cells (Figure 3c, d). Moreover, viral titers of MCs and SKOV3 cells infected at MOI of 3 and HOmMCs infected at MOI of 0.03 increased equally with time. Virus replication was the most efficient in HomMCs; thus these findings suggested that HOmMCs would be suitable for use as carrier cells.

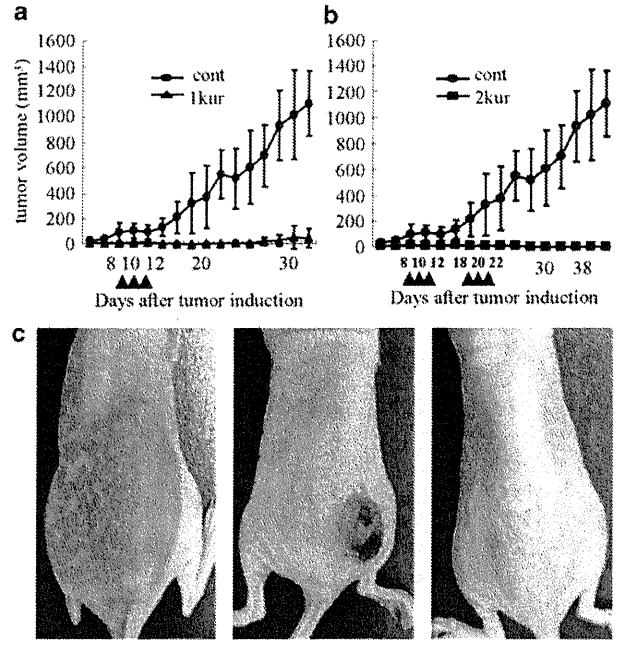


**Figure 2** HF10 reduces tumor growth in a subcutaneous (s.c.) ovarian cancer model. (**a**) In all, $5 \times 10^6$ SKOV3 cells were s.c. implanted into the flank of 5-week-old nude mice. When s.c. tumors were approximately 10–15 mm in diameter, phosphate-buffered saline (PBS) (control) or $1 \times 10^7$ plaque-forming units HF10 were injected intratumorally on days 8, 10 and 12. (**b**) Group two was injected on days 8, 10, 12, 18, 20 and 22. Tumor volume was monitored for the indicated days after treatment ($P<0.01$; control vs HF10 treatment group). Bars represent means + s.e.m. of each group. (**c**) Representative pictures of control (right), group one (middle) and group two (left) at day 30.

### In vitro *delivery of HSV using MCs as carrier cells*

We estimated the efficacy of tumor killing caused by virus-loaded carrier cells *in vitro*. To this end, the oncolytic effects of tumor cells cocultured with virus-loaded MCs was compared with direct infection by virus. We administered Hh101- ($3 \times 10^5$ PFU) or Hh101-infected carrier cells ($1 \times 10^5$ cells; MOI of 3) to the media of SKOV3 cells. At 24 h after infection, virus titers in the media were $6.3 \times 10^4$ PFU ml$^{-1}$ when Hh101-infected carrier cells were administered, and only $2.1 \times 10^2$ PFU ml$^{-1}$ when Hh101 virus was administered. Moreover, CPE was observed ~12 h after infection when Hh101-infected carrier cells were administered (Figure 4a), whereas it was observed 24 h after infection with Hh101 virus alone (Figure 4b). CPE was spread more rapidly and extensively in the case of Hh101-infected carrier cells (Figure 4a). Carrier cells therefore supported sufficient viral replication and could contact target cancer cells efficiently.

### In vitro *immune evasion by cell-based delivery of HSV*

As the majority of human adults has been exposed to HSV and has anti-HSV antibodies, it is theoretically possible that oncolytic virus would be attenuated by circulating antibodies. To examine the effect of antibodies

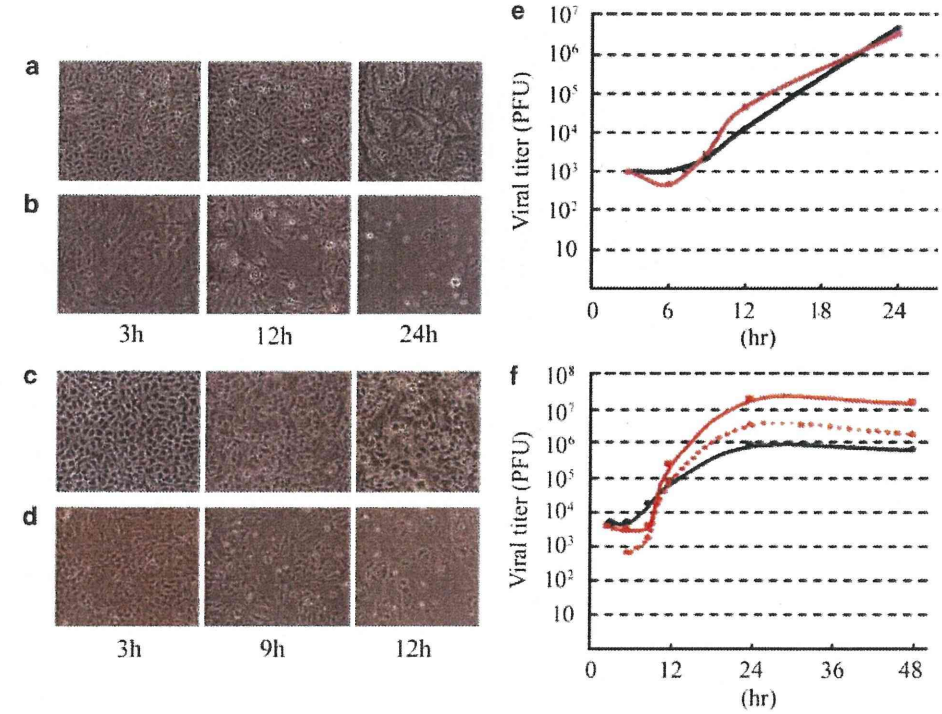


**Figure 3** HF10 and Hh101 replication in mesothelial cells (MCs), human omentum mesothelial cells (HOmMCs) and SKOV3 cells. SKOV3 cells (**a**, black line) and MCs (**b**, red line) were infected with HF10 at multiplicities of infection (MOI) 3. SKOV3 cells (**c**, black line) and HOmMCs (**d**, red line) were infected with Hh101 at MOI 3. Representative cytopathogenic effects (CPE) are shown as time series. Cells were harvested and virus titer was determined by plaque assay. The red dotted line shows virus titers in MCs infected with Hh101 at MOI 0.03 (**e**, **f**). The values represent the mean of samples tested in triplicate. PFU, plaque-forming unit.

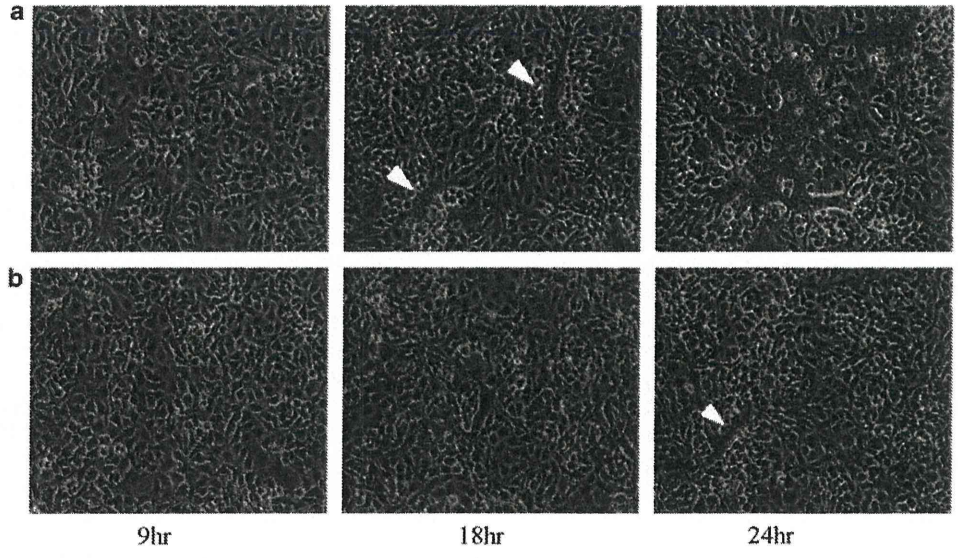


**Figure 4** *In vitro* delivery of herpes simplex virus (HSV) using mesothelial cells as carriers. Hh101-infected carrier cells (**a**) or cell-free Hh101 (**b**) were added to the media of SKOV3 cells. Representative cytopathic effects (CPEs) are shown as time series. The white arrow heads show small CPEs.

against virus delivery by carrier cells, we performed *in vitro* experiments. We plated SKOV3 cells on 35-mm dishes, and after 24 h, HF-GFP ($10^5$ PFU per dish) or HF-GFP-infected carrier cells ($10^4$ cells per dish) were added to the culture media containing with anti-HSV-1 antiserum or control serum. As evidenced by virus-associated fluorescence, extensive replication was seen in SKOV3 cells 24 h following administration of HF-GFP-

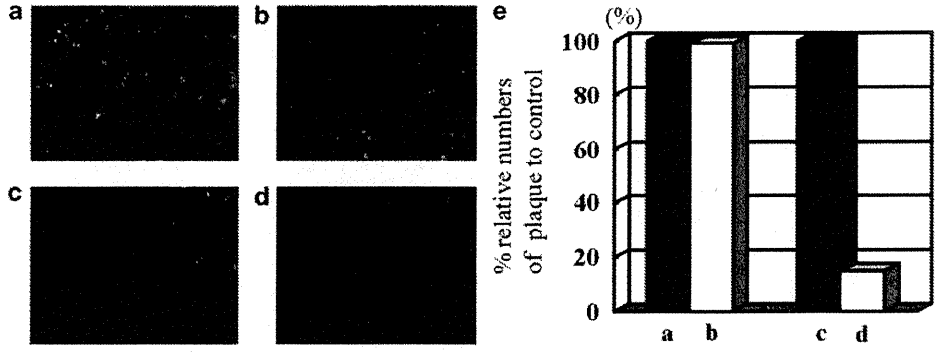


**Figure 5** *In vitro* effects of anti-herpes simplex virus type 1 (HSV-1) antibody on HF-green fluorescent protein (GFP). SKOV3 cells were plated for 24 h, and HF-GFP-infected carrier cells (**a**, **b**) or HF-GFP (**c**, **d**) were added to the media containing control serum (**a**, **c**) or anti-HSV-1 antiserum (**b**, **d**). Anti-HSV-1 antiserum was added to the media to give a final dilution of 1:50. Representative cytopathogenic effect (CPE) images are taken at 24 h using the Leica M205FA fluorescence stereomicroscope with a standard GFP filter set. SKOV3 cells were then fixed, stained with 0.2% crystal violet solution and observed at 30 h. The number of plaques was counted and expressed as a percentage of number obtained in control cultures (**e**).

infected carrier cells in spite of anti-HSV-1 antiserum. In the absence of anti-HSV-1 antiserum (Figure 5a), however, virus-associated fluorescence was larger and brighter than in the presence of anti-HSV-1 antiserum (Figure 5b). In contrast, little virus-associated GFP was observed in SKOV3 cells 24 h following administration of HF-GFP in the presence of anti-HSV-1 antiserum (Figure 5d), although a number of GFP-expressing cells were detectable in the absence of anti-HSV-1 antiserum (Figure 5c). These results indicated that cellular carriers can efficiently shield oncolytic virus from neutralizing antibodies.

### *Localization of virally infected cell delivery in the presence of anti-HSV-1 antiserum*

In order to visualize the distribution of the cellular vehicles in mice, we used HF-GFP, which allowed us to follow the biodistribution of virus-associated fluorescence using an *in vivo* imaging system. To assess the localization of intraperitoneally injected virus, we established a mouse model using ovarian cancer cells, in which $2 \times 10^6$ SKOV3 cells were inoculated into the peritoneal cavity of nude mice, leading to the formation of peritoneal disseminations. HF-GFP was injected into the peritoneal cavity 30 days after the initial inoculation of cancer cells. At 24 h after HF-GFP injection, nearly all visible tumor nodules in the peritoneal cavity were GFP positive. We detected GFP expression even in small tumors and the brightness of GFP varied in each tumor (Figure 6b). In contrast, no GFP expression was seen in the tumors in animals of the control group (Figure 6a). The GFP expression persisted for 7 days after HF-GFP injection; however, the brightness of GFP weakened as time passed. GFP expression persisted longer in mice injected with HF-GFP-infected carrier cells than in mice injected with HF-GFP alone. These findings suggested that viruses injected into the peritoneal cavity exhibited preferential and specific distribution in disseminated cancer foci in HSV-1 naïve animals.

Next, to examine the impact of a pre-existing immune response, we used the passive immunization method in which anti-HSV-1 antiserum was injected i.p. into mice. Intraperitoneal tumor-bearing mice were given cell-free HF-GFP or HF-GFP-infected HOmMCs i.p at 1 h after treatment with anit-HSV-1 antiserum or control serum. No clear GFP signal was observed in disseminated tumors when HF-GFP was given to mice pretreated with anti-HSV-1 antiserum (Figure 6c). In contrast, a significant GFP signal was detected in peritoneal tumors in spite of pretreatment with anti-HSV-1 antiserum, suggesting that infected carrier cells could bypass circulating antibodies and transfer virus to intraperitoneally disseminated ovarian tumors (Figure 6d).

### *Intraperitoneal administration of HSV-1 mutant-infected carrier cells improved survival of mice with ovarian cancer*

To assess the suitability of carrier cells for the delivery of HSV-1 mutants *in vivo*, we conducted survival experiments to compare the effects of Hh101 administered directly with the effects of Hh101 delivered via HOmMCs. Because HF10 is lethal to immunodeficient animals, we utilized Hh101, which is a recombinant virus clone isolated from HF10 and hrR3 and is less virulent than HF10. PBS, Hh101 or Hh101-infected carrier cells were injected three times 3 days after the i.p. injection of $2 \times 10^6$ SKOV3 cells, a time at which tumors would be invisible to the naked eye. Three repeated therapeutic injections of Hh101-infected HOmMCs significantly improved the mean survival time of ovarian cancer-engrafted nude mice (55 days, $n = 10$) compared with the administration of Hh101 alone (46 days, $n = 9$; $P < 0.05$) (Figure 7a). Two-tenth of the animals in the carrier cell-treated group were completely protected from relapse of peritoneal tumor and ascites.

Next, PBS or Hh101-infected carrier cells were injected five times 6 days after the injection of tumor cells, a time at which numerous macroscopic white, 2 mm diameter tumors were seen at the diaphragm, at the mesentery and occasionally at the omentum. As shown in Figure 7b, all mice, irrespective of treatment, developed macroscopic

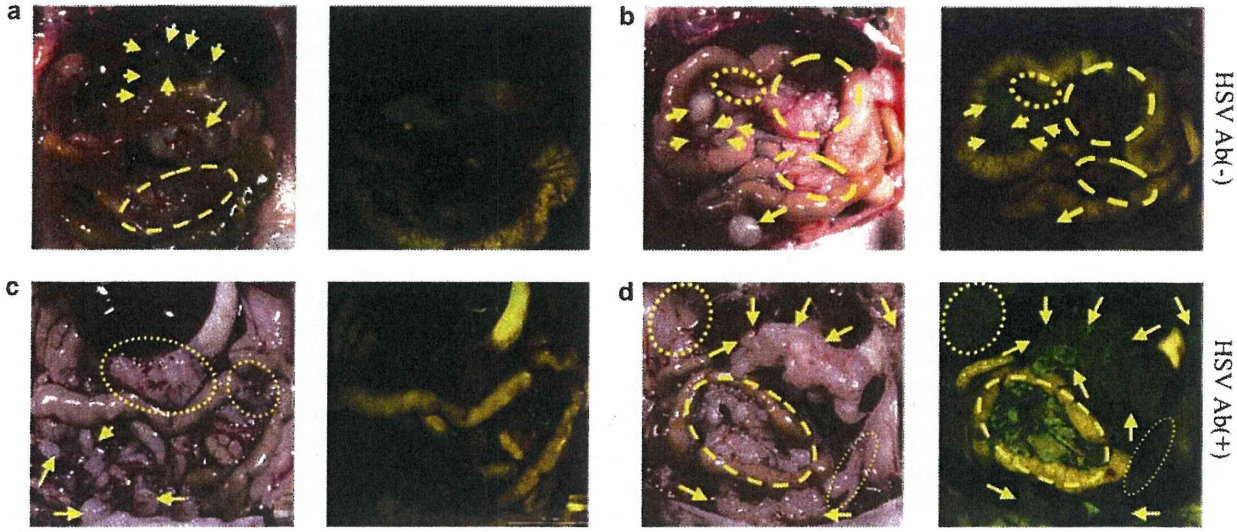


**Figure 6** *In vivo* visualization of virally infected cell delivery in the presence of anti-herpes simplex virus type 1 (HSV-1) antiserum. Mice were bearing disseminated SKOV3 ovarian tumors. Mice were randomized into non-treatment group (**a**, **b**) and treatment group with anti-HSV-1 antiserum (**c**, **d**). Intraperitoneal tumor-bearing mice were given phosphate-buffered saline (PBS) (**a**), cell-free HF-green fluorescent protein (GFP) (**b**, **c**) or HF-GFP-infected human omentum mesothelial cells (HomMCs) (**d**) intraperitoneally 1 h after treatment. Representative photographs showing between tumor location and GFP signal. Each picture taken 24 h after viral injections is shown. The yellow arrows and dotted-line circles indicate disseminated ovarian tumor.

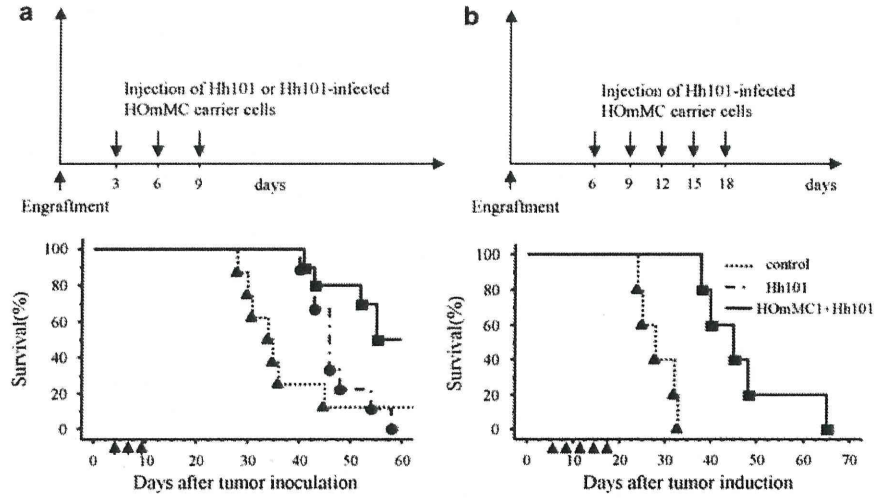


**Figure 7** Therapeutic effects of Hh101-infected carrier cells in an ovarian cancer model. Nude mice were engrafted intraperitoneally with SKOV3 cells and (**a**) treatment was started 3 days later using three repeated i.p. injections. Three repeated therapeutic injections of Hh101-infected human omentum mesothelial cells (HOmMCs) improved the survival of ovarian cancer-engrafted nude mice. Injections of Hh101-infected carrier cells were more effective than Hh101 injections alone. Some of the mice treated with Hh101-infected carrier cells survived without symptoms or site injection tumors for >80 days. (**b**) Therapy was started on day 6 with five repeated i.p. injections. Median survival was significantly ($P=0.0018$) prolonged for the group of carrier-cell-treated animals compared with the control group (median survival, 45 days vs 28 days).

tumors in the peritoneal cavity and subsequently died. However, the survival time was extended by treatment with Hh101-infected carrier cells. This resulted in an approximate doubling of the median survival time (45 days; $n=5$) compared with that for control animals receiving PBS alone (28 days; $n=5$; $P<0.01$). Thus, in both experiments the prognosis was significantly improved by treatment with Hh101-infected carrier cells.

## Discussion

Genetically engineered, conditionally replicating HSV-1 is a promising therapeutic agent for cancer therapy. The main antitumor mechanism of oncolytic viruses results from viral replication within infected tumor cells, resulting in cell destruction, and liberation of progeny virus particles that can directly infect adjacent tumor cells.[7]

Most clinical trials using oncolytic viral therapy have been performed using direct i.t. injection. However, almost all HSV-1 mutants were not so effective as expected when used clinically as antitumor cytolytic agents.[22–24] In an effort to develop more effective, well-tolerated, novel viral therapeutic agents, we have focused a highly attenuated oncolytic HSV-1 mutant, which lacks four accessory genes (*UL56*, *UL43*, *UL49.5* and *UL55*) and LAT (latency-associated transcript).[17–19] Our previous observation have shown that the HF10 is a potent novel agent for oncolytic therapy that is safe and effective for colon cancer, sarcoma and melanoma treatment in mouse models.[25–27] We have also performed a clinical trial of the treatment of recurrent breast cancer and head and neck cancer using i.t. injection of HF10.[28–30] These results revealed a potent oncolytic effect of HF10 without any side effects in human. Currently HF10 is being tested in the United States for the patients with advanced head and neck cancer in a Phase I clinical trial. Here, we have examined the ability of HF10 to control ovarian cancer in order to apply the HF10 therapy for peritoneally disseminated ovarian cancer. Firstly, we performed i.t. therapy of s.c. xenograft tumors using HF10, and tumor growth was significantly reduced. Moreover, in animals treated with six injections, a complete disappearance of the tumor was observed in some animals.

As a strategy to potentially enhance the delivery of HSV to disseminated tumors and to protect the virus from inhibitory factors (complement, anti-HSV antibodies) in the peritoneal cavity, we and others are exploring the use of carrier cells as Trojan Horses to deliver virus to tumors. The optimal carrier cell should be highly susceptible to HSV infection, not be rapidly killed by the virus, traffic to tumors and transfer the viral infection to the tumor cells via cell-to-cell heterofusion and/or by production of virus progeny.[11,31,32] An assortment of cells have been explored in this regard, including tumor cells,[24,33–35] outgrowth endothelial cells[36] and T cells.[31,37] In this work, we observed an ~10-fold higher amplification of the virus in HOmMCs than SKOV3 cells *in vitro*. Virus replication was the most efficient in HOmMCs, so we decided to use these cells as HSV carrier cells. Next, we estimated the efficacy of tumor killing caused by virus-loaded carrier cells *in vitro*. Our *in vitro* studies clearly demonstrated the efficacy of spread of infection between tumor cells and carrier cells. The transfer and spread of infectivity by MCs derived from the omentum was much higher than infectivity transfer by cell-free viruses. Taken together, these findings suggested that HOmMCs would be suitable for use as carrier cells to treat peritoneally disseminated ovarian cancer. However, the ultimate fear of carrier cells after intraperitoneal inoculation may pose some safety concerns. In this study, we immortalized normal human peritoneal MCs with non-viral human genes (mutant Cdk4, cyclin D1 and hTERT) and utilized as carrier cells. Such as the case, a carcinogenic potential of HOmMCs would not emerge thus far (data not shown). In the previous study,[21] we have developed immortalized ovarian surface epithelium with the same gene sets, and we did not observe any tumorigenesis up to doublings 60. The possibility of clinical application of carrier cells warrants that safety would be ensured.

Ascites frequently accumulate in patients who have tumor spread in the peritoneal cavity, and this fluid is expected to be rich in anti-HSV antibodies because the immunoglobulin G content of ascites fluid is known to reflect that of blood.[38] Also, it has been shown that pre-existing neutralizing antibodies in ascites may prevent initial adenovirus vector delivery in ovarian cancer patients.[39] Thus, carrier cells are expected to be useful not only for systemic virus delivery but also for intraperitoneal administration in patients with peritoneal metastases and pre-existing humoral immune response. We also examined the effect of antibodies against virus delivery by carrier cells. Our *in vitro* data demonstrated that direct cell-to-cell transfer of infectivity by HOmMCs was five to six times more resistant to neutralizing antibodies than infectivity transfer by naked virus. Thus, once infection is successfully transferred to the tumor, it is expected that antibodies will not stop i.t. virus spread. We also showed that HOmMCs infected with HF-GFP could target pre-established ovarian tumor nodules in mice (Figure 6), and this result is consistent with that of measles virus-infected cell carriers.[40] These data support the potential use of HSV oncolytic therapy using carrier cells in humans with pre-existing immunity to HSV.

This study supports the concept that the utilization of carrier cells may have a role in HSV-based oncolytic therapies. Inoculation of HOmMCs infected at MOI 3 or the equal titer of HSV particles should represent comparable viral loads initially administered to the animals. In the SKOV3 model, the carrier cell strategy led to a significant prolongation of animal survival compared with virus alone. Earlier treatment (3 days after engraftment) with infected carrier cells was even more effective. Hh101-infected carrier cells rescued few of the animals, because Hh101 is more attenuated than HF10, which is lethal for immunodeficient mice. If we use HF10 for carrier cell-based therapy in an immunocompetent model, we anticipate that the therapeutic effect would be better and be enhanced. Moreover, the immunogenicity of carrier cells may enhance therapy, as the activation of antitumor immunity during virotherapy appears to contribute to some degree to eliminating tumors and may help to protect from disease. To estimate the role of the immune response in oncolytic viral therapy, we would need to investigate this theory in a syngeneic immunocompetent mouse model of disseminated peritoneal ovarian carcinoma.

In conclusion, we establish that human peritoneal MCs are useful for carrier cells of oncolytic HSV in treating peritoneally disseminated ovarian cancer. Infected MCs and HOmMCs have the unique ability to produce a burst of virus upon delivery to the tumor site. In addition, this strategy allowed oncolytic HSV to escape neutralization by antibodies and complement, and subsequently to transfer the virus to tumor cells by *in situ* cell fusion. These findings may have significant implications for oncolytic virotherapy for ovarian cancer.

## Conflict of interest

The authors declare no conflict of interest.

## Acknowledgements

This study was supported, in part, by a research grant (number 21592128) from the Ministry of Education, Science and Culture of Japan.

## References

1 Ushijima K. Current status of gynecologic cancer in Japan. *J Gynecol Oncol* 2009; **20**: 67–71.
2 DiSaia PJ, Tewari KS. Recent advancements in the treatment of epithelial ovarian cancer. *J Obstet Gynaecol Res* 2001; **27**: 61–75.
3 Chiocca EA. Oncolytic viruses. *Nat Rev Cancer* 2002; **2**: 938–950.
4 Ichikawa T, Chiocca EA. Comparative analyses of transgene delivery and expression in tumors inoculated with a replication-conditional or -defective viral vector. *Cancer Res* 2001; **61**: 5336–5339.
5 Parato KA, Senger D, Forsyth PA, Bell JC. Recent progress in the battle between oncolytic viruses and tumours. *Nat Rev Cancer* 2005; **5**: 965–976.
6 Liu TC, Kirn D. Systemic efficacy with oncolytic virus therapeutics: clinical proof-of-concept and future directions. *Cancer Res* 2007; **67**: 429–432.
7 Nomura N, Kasuya H, Watanabe I, Shikano T, Shirota T, Misawa M *et al.* Considerations for intravascular administration of oncolytic herpes virus for the treatment of multiple liver metastases. *Cancer Chemother Pharmacol* 2009; **63**: 321–330.
8 Kasuya H, Pawlik TM, Mullen JT, Donahue JM, Nakamura H, Chandrasekhar S *et al.* Selectivity of an oncolytic herpes simplex virus for cells expressing the DF3/MUC1 antigen. *Cancer Res* 2004; **64**: 2561–2567.
9 Mullen JT, Kasuya H, Yoon SS, Carroll NM, Pawlik TM, Chandrasekhar S *et al.* Regulation of herpes simplex virus 1 replication using tumor-associated promoters. *Ann Surg* 2002; **236**: 502–512, discussion 512-3.
10 Hashido M, Lee FK, Nahmias AJ, Tsugami H, Isomura S, Nagata Y *et al.* An epidemiologic study of herpes simplex virus type 1 and 2 infection in Japan based on type-specific serological assays. *Epidemiol Infect* 1998; **120**: 179–186.
11 Iankov ID, Blechacz B, Liu C, Schmeckpeper JD, Tarara JE, Federspiel MJ *et al.* Infected cell carriers: a new strategy for systemic delivery of oncolytic measles viruses in cancer virotherapy. *Mol Ther* 2007; **15**: 114–122.
12 Power AT, Wang J, Falls TJ, Paterson JM, Parato KA, Lichty BD *et al.* Carrier cell-based delivery of an oncolytic virus circumvents antiviral immunity. *Mol Ther* 2007; **15**: 123–130.
13 Croyle MA, Chirmule N, Zhang Y, Wilson JM. PEGylation of E1-deleted adenovirus vectors allows significant gene expression on readministration to liver. *Hum Gene Ther* 2002; **13**: 1887–1900.
14 Green NK, Herbert CW, Hale SJ, Hale AB, Mautner V, Harkins R *et al.* Extended plasma circulation time and decreased toxicity of polymer-coated adenovirus. *Gene Ther* 2004; **11**: 1256–1263.
15 Ilett EJ, Prestwich RJ, Kottke T, Errington F, Thompson JM, Harrington KJ *et al.* Dendritic cells and T cells deliver oncolytic reovirus for tumour killing despite pre-existing anti-viral immunity. *Gene Ther* 2009; **16**: 689–699.
16 Power AT, Bell JC. Taming the Trojan horse: optimizing dynamic carrier cell/oncolytic virus systems for cancer biotherapy. *Gene Ther* 2008; **15**: 772–779.
17 Nishiyama Y, Kimura H, Daikoku T. Complementary lethal invasion of the central nervous system by nonneuroinvasive herpes simplex virus types 1 and 2. *J Virol* 1991; **65**: 4520–4524.
18 Ushijima Y, Luo C, Goshima F, Yamauchi Y, Kimura H, Nishiyama Y. Determination and analysis of the DNA sequence of highly attenuated herpes simplex virus type 1 mutant HF10, a potential oncolytic virus. *Microbes Infect* 2007; **9**: 142–149.
19 Yamada Y, Kimura H, Morishima T, Daikoku T, Maeno K, Nishiyama Y. The pathogenicity of ribonucleotide reductase-null mutants of herpes simplex virus type 1 in mice. *J Infect Dis* 1991; **164**: 1091–1097.
20 Kajiyama H, Kikkawa F, Maeda O, Suzuki T, Ino K, Mizutani S. Increased expression of dipeptidyl peptidase IV in human mesothelial cells by malignant ascites from ovarian carcinoma patients. *Oncology* 2002; **63**: 158–165.
21 Sasaki R, Narisawa-Saito M, Yugawa T, Fujita M, Tashiro H, Katabuchi H *et al.* Oncogenic transformation of human ovarian surface epithelial cells with defined cellular oncogenes. *Carcinogenesis* 2009; **30**: 423–431.
22 Coukos G, Makrigiannakis A, Montas S, Kaiser LR, Toyozumi T, Benjamin I *et al.* Multi-attenuated herpes simplex virus-1 mutant G207 exerts cytotoxicity against epithelial ovarian cancer but not normal mesothelium and is suitable for intraperitoneal oncolytic therapy. *Cancer Gene Ther* 2000; **7**: 275–283.
23 Yoon SS, Carroll NM, Chiocca EA, Tanabe KK. Cancer gene therapy using a replication-competent herpes simplex virus type 1 vector. *Ann Surg* 1998; **228**: 366–374.
24 Coukos G, Makrigiannakis A, Kang EH, Caparelli D, Benjamin I, Kaiser LR *et al.* Use of carrier cells to deliver a replication-selective herpes simplex virus-1 mutant for the intraperitoneal therapy of epithelial ovarian cancer. *Clin Cancer Res* 1999; **5**: 1523–1537.
25 Kimata H, Takakuwa H, Goshima F, Teshigahara O, Nakao A, Kurata T *et al.* Effective treatment of disseminated peritoneal colon cancer with new replication-competent herpes simplex viruses. *Hepatogastroenterology* 2003; **50**: 961–966.
26 Takakuwa H, Goshima F, Nozawa N, Yoshikawa T, Kimata H, Nakao A *et al.* Oncolytic viral therapy using a spontaneously generated herpes simplex virus type 1 variant for disseminated peritoneal tumor in immunocompetent mice. *Arch Virol* 2003; **148**: 813–825.
27 Watanabe D, Goshima F, Mori I, Tamada Y, Matsumoto Y, Nishiyama Y. Oncolytic virotherapy for malignant melanoma with herpes simplex virus type 1 mutant HF10. *J Dermatol Sci* 2008; **50**: 185–196.
28 Kimata H, Imai T, Kikumori T, Teshigahara O, Nagasaka T, Goshima F *et al.* Pilot study of oncolytic viral therapy using mutant herpes simplex virus (HF10) against recurrent metastatic breast cancer. *Ann Surg Oncol* 2006; **13**: 1078–1084.
29 Nakao A, Kimata H, Imai T, Kikumori T, Teshigahara O, Nagasaka T *et al.* Intratumoral injection of herpes simplex virus HF10 in recurrent breast cancer. *Ann Oncol* 2004; **15**: 988–989.
30 Teshigahara O, Goshima F, Takao K, Kohno S, Kimata H, Nakao A *et al.* Oncolytic viral therapy for breast cancer with herpes simplex virus type 1 mutant HF 10. *J Surg Oncol* 2004; **85**: 42–47.

31 Ong HT, Hasegawa K, Dietz AB, Russell SJ, Peng KW. Evaluation of T cells as carriers for systemic measles virotherapy in the presence of antiviral antibodies. *Gene Ther* 2007; **14**: 324–333.
32 Peng KW, Dogan A, Vrana J, Liu C, Ong HT, Kumar S *et al.* Tumor-associated macrophages infiltrate plasmacytomas and can serve as cell carriers for oncolytic measles virotherapy of disseminated myeloma. *Am J Hematol* 2009; **84**: 401–407.
33 Garcia-Castro J, Martinez-Palacio J, Lillo R, Garcia-Sanchez F, Alemany R, Madero L *et al.* Tumor cells as cellular vehicles to deliver gene therapies to metastatic tumors. *Cancer Gene Ther* 2005; **12**: 341–349.
34 Power AT, Bell JC. Cell-based delivery of oncolytic viruses: a new strategic alliance for a biological strike against cancer. *Mol Ther* 2007; **15**: 660–665.
35 Raykov Z, Balboni G, Aprahamian M, Rommelaere J. Carrier cell-mediated delivery of oncolytic parvoviruses for targeting metastases. *Int J Cancer* 2004; **109**: 742–749.
36 Jevremovic D, Gulati R, Hennig I, Diaz RM, Cole C, Kleppe L *et al.* Use of blood outgrowth endothelial cells as virus-producing vectors for gene delivery to tumors. *Am J Physiol Heart Circ Physiol* 2004; **287**: H494–H500.
37 Cole C, Qiao J, Kottke T, Diaz RM, Ahmed A, Sanchez-Perez L *et al.* Tumor-targeted, systemic delivery of therapeutic viral vectors using hitchhiking on antigen-specific T cells. *Nat Med* 2005; **11**: 1073–1081.
38 Confino E, Harlow L, Gleicher N. Peritoneal fluid and serum autoantibody levels in patients with endometriosis. *Fertil Steril* 1990; **53**: 242–245.
39 Stallwood Y, Fisher KD, Gallimore PH, Mautner V. Neutralisation of adenovirus infectivity by ascitic fluid from ovarian cancer patients. *Gene Ther* 2000; **7**: 637–643.
40 Mader EK, Maeyama Y, Lin Y, Butler GW, Russell HM, Galanis E *et al.* Mesenchymal stem cell carriers protect oncolytic measles viruses from antibody neutralization in an orthotopic ovarian cancer therapy model. *Clin Cancer Res* 2009; **15**: 7246–7255.

Virology 422 (2012) 99–104

Contents lists available at SciVerse ScienceDirect

Virology

journal homepage: www.elsevier.com/locate/yviro

# Molecular cloning and characterization of a novel human papillomavirus, HPV 126, isolated from a flat wart-like lesion with intracytoplasmic inclusion bodies and a peculiar distribution of Ki-67 and p53

Nagayasu Egawa [a], Kazuhiro Kawai [b], Kiyofumi Egawa [c,d], Yumi Honda [e], Takuro Kanekura [b], Tohru Kiyono [a,*]

[a] Division of Virology, National Cancer Center Research Institute, Tokyo, Japan
[b] Department of Dermatology, Kagoshima University Graduate School of Medical and Dental Sciences, Kagoshima, Japan
[c] Department of Dermatology, The Jikei University School of Medicine, Tokyo, Japan
[d] Department of Microbiology, Kitasato University School of Allied Health Science, Sagamihara, Japan
[e] Department of Surgical Pathology, Kumamoto University Hospital, Kumamoto, Japan

ARTICLE INFO

*Article history:*
Received 9 August 2011
Accepted 10 October 2011
Available online 5 November 2011

*Keywords:*
Human papillomavirus type 126
Gamma papillomavirus
Flat warts
Adult T-cell leukemia
Ki-67
p53
Homogeneous intracytoplasmic inclusion body (Hg-ICB)

ABSTRACT

Infection with certain human papillomavirus types induces warts with specific macroscopic and microscopic features. We observed multiple flat wart-like lesions on the chest, neck and extremities of an adult T-cell leukemia patient. Histologically, atypical intracytoplasmic inclusion bodies currently known to be pathognomonic for genus gamma or mu papillomaviruses were disclosed in some cells of the epidermis showing histological features compatible with flat warts. In the present study, a novel human papillomavirus was identified and its whole genome, 7326 bp in length, was cloned and characterized. Phylogenetic analysis showed the virus designated as HPV126 to be a novel type of genus gamma papillomavirus. Strikingly, Ki-67 and p53 expression was found to be increased in all layers of the epidermis except for horny layer, contrasting to expression restricted to the basal and lower spinous layers in ordinary flat warts.



## Introduction

So far, more than one hundred twenty human papillomaviruses (HPVs) have been characterized based on nucleotide sequence diversity (Bernard et al., 2010). Infections of distinct types of HPVs are characterized by type-specific cytopathic/cytopathogenic effects (CPEs), i.e., macro- and microscopic features, pathological properties, and tissue tropisms. Hence, unusual CPEs which had not previously been described may suggest that lesions could be induced by a novel type of HPV (Egawa, 2005). We recently observed intracytoplasmic inclusion bodies (ICBs) resembling the HPV 4/60/65-associated homogenous ICB (Hg-ICB) (Egawa, 1994, 2005; Egawa et al., 1993) in flat wart-like lesions of a patient with adult T-cell leukemia (ATL). However, the clinical features of the lesions proved quite different from those of HPV 4/60/65-associated skin lesions, i.e., pigmented warts (Egawa, 1988; Egawa et al., 1993) or ridged warts (Honda et al., 1994), suggesting the presence of a previously unidentified papillomavirus. While the HPV type-specific CPEs are important in understanding the biological nature of the viruses, many of the novel HPV genotypes recently isolated lacked specific cell biological aspects.

The present report describes not only isolation and molecular biological characterization of a novel HPV genotype, HPV126, but also a clinical, histopathological and immunohistochemical characterization of HPV 126-associated skin lesions, revealing this novel human genus gamma papillomavirus to induce flat wart-like lesions with Hg-ICBs. Strikingly, Ki-67 and p53, well-known cell cycle proteins, were established to be expressed in all layers of the epidermis except for horny layer in the lesions, quite different from the expression pattern restricted to basal and lower spinous layers seen in ordinary flat warts.

## Results

### *Histopathological features of wart lesions*

Disseminated hypopigmented macules clinically resembling flat warts or epidermodysplasia verruciformis-related tinea versicolor-like lesions (Jablonska and Orth, 1985) were seen on the chest, neck, and extremities of a 56-year-old Japanese patient (Fig. 1A) (Kawai et al., 2009). A biopsy was taken from the disseminated fused lesion and adjacent normal-looking skin. Microscopically, at least two independent wart-

* Corresponding author at: Division of Virology, National Cancer Center Research Institute, 5-1-1 Tsukiji, Tyuo-ku, Tokyo 104-0045, Japan. Fax: +81 3 3543 2181.
*E-mail address:* tkiyono@ncc.go.jp (T. Kiyono).

0042-6822/$ – see front matter © 2011 Elsevier Inc. All rights reserved.
doi:10.1016/j.virol.2011.10.011

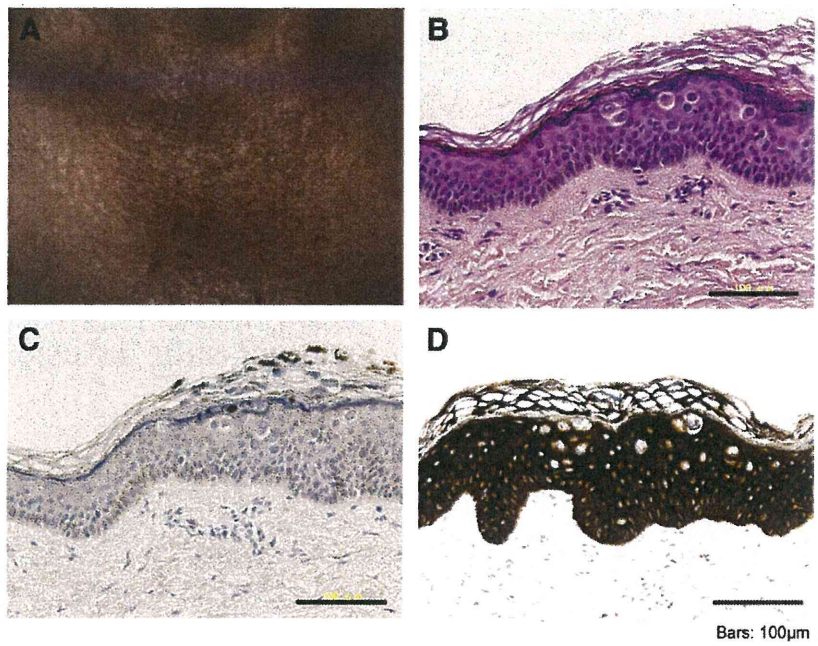


**Fig. 1.** Clinical (A), histopathological (B) and immunohistochemical (C and D) findings for the HPV 126-associated flat wart-like lesion. Macroscopic appearance of the flat wart-like lesions (A). In contrast to the normal skin adjacent to the flat wart-like lesion, Hg-ICBs are evident in balloon cells in the upper epidermal cell layers (B); strong positive signals for papillomavirus common antigen (L1 protein) in the nuclei of the cells in horny layer and cells with Hg-ICBs in granular layer (C); and positive signals for pan-cytokeratin are lacking in the cells with ICB (D). Scale bars; 100 μm.

like lesions separated by normal epidermis were included in the specimen. The epidermis showed mild acanthosis with basket-weave-like hyperkeratosis, partial hypergranulosis and mild papillomatosis, basic histological features compatible with those of flat warts (Fig. 1B) (Jablonska et al., 1985). However, additional unique histopathological features were also seen, i.e., keratinocytes with an enlarged nucleus, abundant blue-gray cytoplasm, occasional perinuclear haloes, and prominent keratohyalin granules observed in the granular and spinous layers, which are histopathological features consistent with EV (Jablonska and Orth, 1985). In addition, large clear cells contained homogeneous eosinophilic ICBs (Fig. 1B) resembling the homogeneous ICBs (Hg-ICBs) previously described in HPV 4/60/65-associated cutaneous warts (Egawa, 1994, 2005; Egawa et al., 1993) .

*Cloning and characterization of the HPV 126 genome*

Although highly sensitive PCR failed to detect the DNA of either genus beta or mu papillomaviruses from the frozen biopsy specimen, a segment of a putative novel type genus gamma papillomavirus was amplified with a gamma papillomavirus-specific degenerate primers (Kawai et al., 2009) (Supplementary Fig. 1). Based on the nucleotide sequence, the full genome was cloned as described in Materials and methods. Sequencing of two clones from independent PCR reactions revealed the full genome consists of 7326 bp in length with a GC content of 50.5%. With a cutaneotropic papillomavirus primer set FAP59/FAP64 (Forslund et al., 1999), only the corresponding region of the cloned genome was amplified, further indicating the HPV is a single type in the lesions of this patient. The cloned HPV was found to be closely related to genus gamma papillomavirus types with an L1 ORF nucleotide similarity ranging from 60.1% to 68.7% (Table 1). According to the established criteria for a new type of papillomavirus that a new type should have 10% divergence of the L1 ORF nucleotide sequence from that of any other papillomavirus type {de Villiers, 2004 #16}, the cloned HPV qualified as a new type of papillomavirus designated as HPV126. According to the proposed criteria for species that should share between 60% and 70% nucleotide identity within a genus, we propose that HPV126, which has less than 70% nucleotide identity with any other papillomaviruses, constitutes a new species of genus gamma papillomavirus. Generation of a phylogenetic tree based on complete L1 nucleotide sequences of representative HPV types indicated that HPV 126 is most closely related to HPV 129 (Fig. 3), with similarity of 68.7% (Table 1). HPV 126 has a typical genomic organization for a genus gamma papillomavirus, and it has seven ORFs, E6, E7, E1, E2, E4, L2 and L1, but no E5 (Supplementary Fig. 2).

*Immunohistochemical features of the wart lesions*

Strong signals of L1 capsid proteins were seen in the nuclei of the cells in horny layer and cells with the ICBs in granular layer (Fig. 1C), suggesting active production of virions. In the cells with ICBs, little cytokeratin staining was observed while strong staining was observed in all epidermal cell layers of the lesions as well as its adjacent normal skin (Fig. 1D).

**Table 1**
Nucleotide sequence pairwise comparison of HPV 126 ORFs with those of representative genus gamma papillomaviruses.

| ORF / HPV type | E6 | E7 | E1 | E2 | E4 | L1 | L2 |
|---|---|---|---|---|---|---|---|
| HPV 4 | 52.2 | 53.2 | 66.2 | 57.3 | 57.3 | 63.5 | 51.6 |
| HPV 48 | 54.0 | 60.3 | 61.3 | 55.6 | 52.7 | 61.4 | 52.7 |
| HPV 50 | 49.1 | 55.9 | 61.6 | 58.5 | 55.2 | 61.5 | 52.7 |
| HPV 60 | 54.3 | 54.0 | 65.5 | 59.8 | 59.5 | 62.9 | 53.6 |
| HPV 65 | 53.4 | 50.5 | 67.0 | 54.7 | 55.0 | 61.4 | 51.9 |
| HPV 88 | 51.5 | 55.4 | 64.5 | 57.1 | 55.6 | 62.8 | 52.6 |
| HPV 95 | 52.6 | 51.5 | 66.9 | 57.2 | 57.5 | 62.2 | 52.6 |
| HPV 112 | 55.0 | 53.0 | 61.0 | 58.4 | 53.7 | 62.4 | 50.4 |
| HPV 116 | 60.3 | 53.7 | 66.4 | 60.9 | 58.6 | 67.6 | 57.7 |
| HPV 119 | 52.5 | 53.4 | 62.0 | 58.3 | 52.9 | 61.5 | 50.3 |
| HPV 121 | 55.0 | 55.1 | 63.8 | 55.8 | 53.4 | 63.1 | 52.3 |
| HPV 123 | 47.1 | 48.0 | 60.5 | 55.6 | 51.4 | 60.1 | 51.6 |
| HPV 129 | 58.3 | 57.4 | 67.3 | 60.2 | 61.1 | 68.7 | 58.7 |

Similarities (%). Sequence for the genus gamma papillomaviruses were obtained from GenBank.

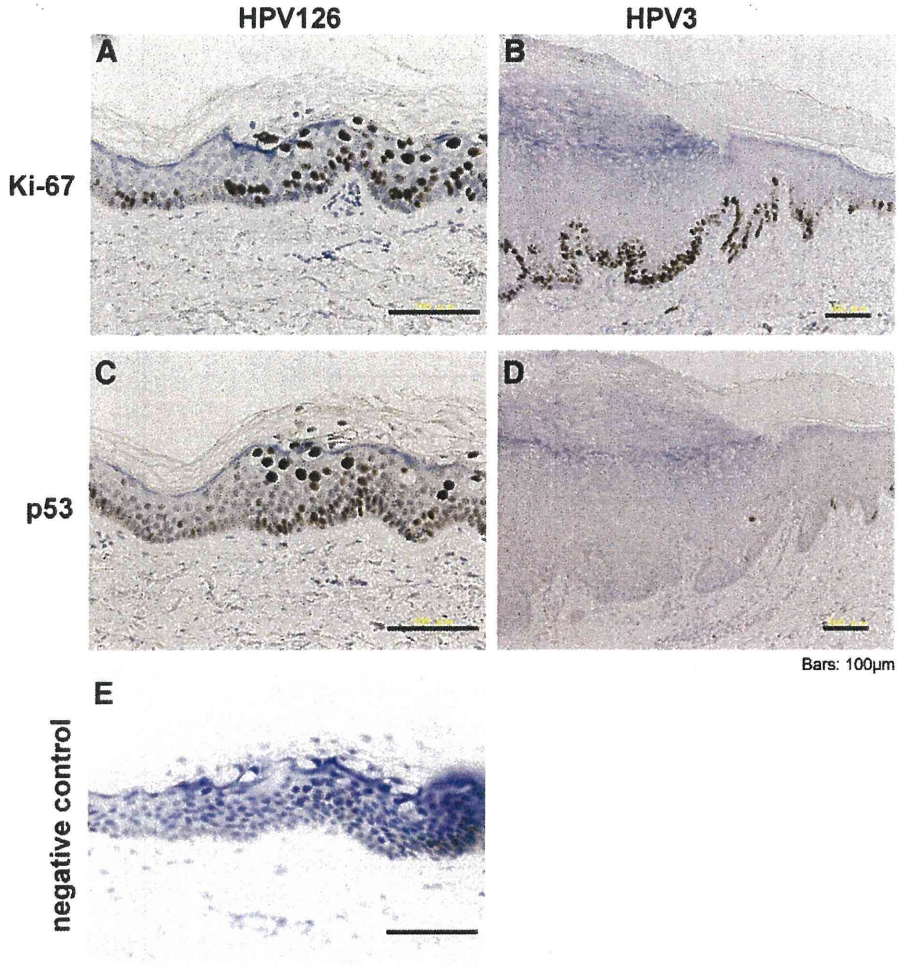


**Fig. 2.** Immunohistochemical features of the HPV 126-associated flat wart-like lesion. In contrast to the normal skin adjacent to the flat wart-like lesion (left side), positive signals for both Ki-67 (A) and p53 (C) are apparent in all compartments of the epithelium except for horny layer of the lesion (right side). However, a divergence is seen between Ki-67 and p53 staining. In contrast to that strong staining for Ki-67 is seen parabasal cells as well as cells of upper epidermal layers, the strong signal is seen predominantly in cells of upper epidermal cell layers. In contrast, weak (B) and faint (D) signals are restricted to the basal and parabasal (B) or lower spinous (D) layers of typical HPV 3-associated flat warts. Scale bars; 100 μm. As a negative control, no signals are observed in the staining of normal non-immune serum from the same source as the primary antibody (E).

Increased expression of Ki-67, an indicative marker of cycling cells, was observed in all compartments of the epithelium except for horny layer of the lesions, whereas its expression was restricted to the basal proliferative compartment of the adjacent normal epidermis (Fig. 2A) and to basal to parabasal cells in the typical HPV 3-positive flat warts (Fig. 2B).

Increased p53 staining was also observed in all compartments of the epithelium except for horny layer of the lesions in the HPV 126-associated lesions. However, unlike Ki-67, strong signals were not seen in parabasal cells for p53. In the adjacent normal epidermis, weak staining for p53 was restricted to the basal proliferative compartment (Fig. 2C), and faint staining was in the basal and lower spinous layers in HPV 3-positive typical flat warts (Fig. 2D). Five cases of typical HPV 3-associated flat warts were examined for comparison to confirm the unusual distribution of Ki-67 and p53 expression in the present flat wart-like lesion though the present case is the only patient with HPV 126-asssociated inclusion warts studied thus far. These observations are reminiscence of high grade cervical intraepithelial neoplasia. However, neither the HPV 126-associated flat wart-like lesions nor ordinary flat warts showed positive staining for $p16^{INK4a}$, while cervical cancer biopsy examined as a positive control exhibited strong positive signals (data not shown).

## Discussion

In the present study, the full-length genome of a novel papillomavirus, HPV 126, was cloned from flat wart-like lesions arising in a Japanese ATL patient and characterized. The DNA genome of HPV 126 consists of 7326 base pairs and shows the gene arrangement characteristic for a cutaneous HPV. The nucleotide sequence of the L1 ORF of HPV 126 shares the highest homology of 68.7% to that of HPV 129, a genus gamma papillomavirus, thereby defining HPV 126 a novel type possibly constituting a novel species of the genus gamma papillomavirus (de Villiers et al., 2004). The HPV 126-associated cutaneous lesions on the chest, neck and extremities of our Japanese ATL patient were disseminated hypopigmented macules clinically resembling flat warts or tinea versicolor-like lesions seen in epidermodysplasia verruciformis (EV) and acquired EV patients (Jablonska and Orth, 1985; Lutzner et al., 1983).

On microscopy balloon cells with pale blue cytoplasm like those seen in flat wart-like lesions of EV or acquired EV patients (Jablonska and Orth, 1985; Lutzner et al., 1983). Additional features characteristic for the present case were ICBs most resemble those associated with HPV 4/60/65, which are members of species 1 (HPV 4/65) and species 4 (HPV 60) of genus gamma papillomaviruses. (Egawa,

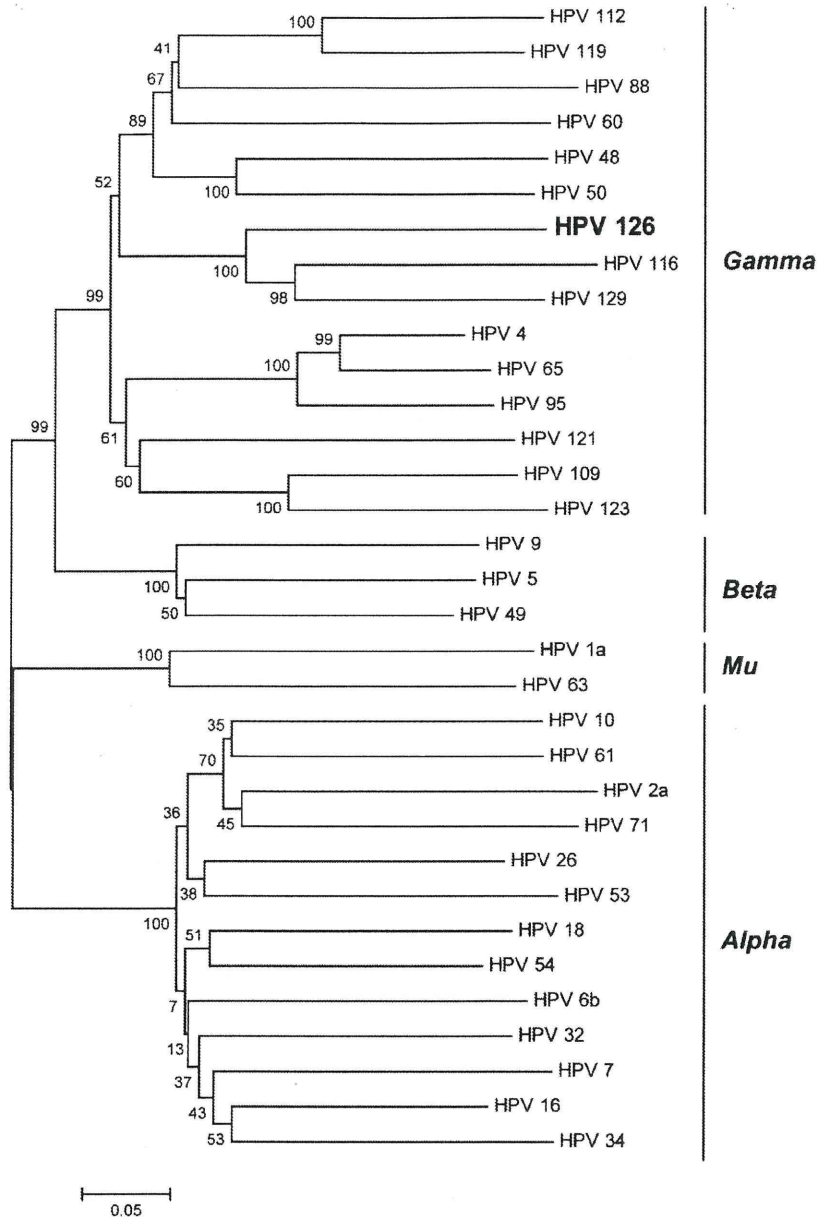


**Fig. 3.** Phylogenic relationships among HPV 126 and representative HPV types. A phylogenetic tree was constructed based on L1 ORF sequences using the neighbor-joining (NJ) method with 1000 bootstrap replicates. Numbers near branches indicate support index from NJ bootstrap percentage. Nucleotide sequences of representative HPVs were obtained from GenBank.

1994, 2005, 2007; Egawa et al., 1993). It is well known that distinct ICBs are pathognomonic for genus gamma and mu papillomaviruses (Egawa, 2007), although the histological features of recently isolated genus gamma papillomaviruses, including HPV 129 and HPV 116, have yet to be described (Bernard et al., 2010; Li et al., 2009). Cytokeratins were absent from cells containing Hg-ICBs (Fig. 1D), in which E4 proteins are thought to be a major component, though E4 protein expression was not examined in the present case. Thus like HPV16 E4 (Doorbar et al., 1989), HPV 126 E4 might be involved in interference with keratin filament assembly.

Another striking feature of the present case was its peculiar immunohistochemical localization of Ki-67 and p53, namely, they were expressed strongly and distributed in all compartments of the epithelium except for horny layer of the HPV 126-associated lesions (Fig. 2). Antigen Ki-67 is expressed during all phases of the cellular cycle, G1, S, G2, and M, of proliferating cells, but is absent in quiescent cells (G0). It is, therefore, a marker of cellular proliferation, which can be detected with monoclonal antibodies. Interaction of human papillomavirus oncoproteins E6 and E7 with cell cycle proteins leads to disturbance of the cell cycle and subsequent alteration in expression of some cell cycle proteins, such as $p16^{INK4a}$, cyclin D1, p53 and Ki-67. Abrupt inactivation of pRB can induce p53 accumulation though activation $p14^{ARF}$ (Bates et al., 1998). Like other HPVs, E7 protein of HPV 126 conserves the pRB binding motif and potentially inactivates pRB. Indeed some of the E7 proteins of cutaneous HPVs, such as HPV1 E7, can strongly bind and inactivate pRB (Hiraiwa et al., 1996; Schmitt et al., 1994). Thus it will be interesting to examine the activity of HPV 126 E7 protein and relationship among expression levels of HPV 126 E7, Ki-67 and the p53 accumulation. Unlike high grade CIN lesions where a positive correlation between the expression of the $p16^{INK4a}$

and Ki-67 has been reported (Nam et al., 2008; Queiroz et al., 2006), accumulation of $p16^{INK4a}$ was not detected in the Ki-67 positive cells (data not shown) in the present case whose clinical behavior and histopathological findings were benign (Kawai et al., 2009).

In conclusion, HPV 126, isolated and characterized in the present study, is a novel type of genus gamma papillomavirus and associated with flat wart- or EV-related tinea versicolor-like clinical features: histological ICBs as with other genus gamma papillomaviruses; and immunohistochemical expression of Ki-67 and p53 in characteristic manner not typical for benign cutaneous warts. It is probable that conditions accompanying immunosuppression in this ATL patient may have contributed to stimulate viral production of HPV 126, thus leading to wart formation, as known for acquired EV (Lutzner et al., 1983). To ascertain the true nature of HPV 126 and its associated warts, we need to perform epidemiological as well as further clinicopathological and virological studies on a larger number of lesions and patients, including immunocompromised individuals.

## Materials and methods

### *Patient*

A 56-year-old Japanese man was referred to us in August 2008 for evaluation of a 5-year history of disseminated hypopigmented macules clinically resembling flat warts or epidermodysplasia verruciformis-related tinea versicolor-like lesions (Jablonska and Orth, 1985) on the chest, neck, and extremities (Fig. 1A) (Kawai et al., 2009). The patient might have been suffering from immunodeficiency, because he was diagnosed as having chronic type of adult T-cell leukemia at the age of 52 years and manifested recurrent fungal pneumonia, rapidly progressing oral squamous cell carcinoma and multiple brain abscesses. A biopsy specimen was taken from the flat wart-like lesions with adjacent normal skin under suspicion of acquired EV (Lutzner et al., 1983). The biopsy specimen was cut into two pieces, one of which was fixed in 20% buffered formalin and embedded in paraffin for conventional histopathological and immunohistochemical analyses, and the other was frozen and stored in −70 °C for further analyses including DNA extraction.

### *Microscopical examination*

Four-micrometer thick sections were obtained from the formalin-fixed and paraffin-embedded biopsy specimen, stained with hematoxylin and eosin (H&E), and examined microscopically.

### *Cloning and characterization of HPV DNA*

Degenerate primers to detect genus gamma papillomaviruses were as described previously (Kawai et al., 2009). The amplified sequence turned out to correspond to nt 4641 to 5632 of the cloned HPV126 (Supplementary Fig. 1). Then abutting primers were designed juxtaposing the *Hpa*I site present in the L1 region (forward primer: 5′-GTTAACAGTAGGCCATCCCTATTTTGATATTGTTG-3′, reverse primer: 5′-GTTAACAGTCTTTCAGTATTTGCATGAAAATAAATATCG-3′). The genome was amplified by 30 cycles of PCR using KOD plus DNA polymerase (Toyobo, Japan) according to the supplier's instruction; annealing at 60 °C, elongation at 68 °C for 8 min. About 8 kbp PCR products were purified and then cloned into pBluescriptIISK(−) (Stratagene, La Jolla, CA), in which 15-bp overlapping sequence of HPV 126 was added to the *Not*I site by PCR (forward primer: 5′-TGAAAGACTGTTAACGCGG-CCGCTCTAGAACTAGTGGATC-3′, reverse primer: 5′-TGGCCTACTGT-TAACGCGGCCGCCACCGCGGTGGAGCTCC-3′), by In-Fusion reaction (Clontech, Mountain View, CA). The complete genomic sequence of a clone was initially determined using primer walking by Nihon Gene Research Laboratories Inc. With the same set of primers (Supplementary Table 1), we confirmed the sequence of another clone from an independent PCR reaction to be identical (Supplementary Fig. 1). The DNA clone was submitted to the Human Papillomavirus Reference Laboratory (Heidelberg, Germany) for official designation, HPV 126, and the sequence was reconfirmed. HPV 126 sequence was submitted to DNA Data Bank of Japan (DDBJ) under accession number AB646346. Nucleotide sequence pairwise comparison of HPV 126 ORFs with types representing genus gamma papillomaviruses and L1 nucleotide global multiple sequence alignments were analyzed using ClustalW program (Thompson et al., 1994). Each gap was included and counted as one position. Phylogenetic analyses were conducted using MEGA version 4 (Tamura et al., 2007).

### *Immunohistochemical examination*

Formalin-fixed and paraffin-embedded tissue sections (4 μm-thick) were deparaffinized in xylene and rehydrated through a series of graded ethanols (100–70%). For antigen retrieval, slides were immersed in citrate buffer (pH6.0) and were heated for 20 min in a microwave. The slides were then incubated in methanol containing 0.3% $H_2O_2$ to inhibit endogenous peroxidase activity. After washing, primary antibodies (Anti-papillomavirus common antigen, DAKO, clone K1H8, 1:200; Ki-67, DAKO, Clone MIB-1, 1:50; p53 protein, DAKO, Clone DO-7, 1:50; $p16^{INK4a}$, Santa Cruz, Clone JC8, 1:200; cytokeratin, Nichirei, polyclonal,1:2) were applied for 1 h and binding was detected using an Envision Kit (Dako Cytomation; K4006). Color development was achieved with 3, 3-diaminobenzine (DAB) as the chromogen and hematoxylin counterstaining was performed to aid in orientation. As a negative control, normal non-immune serum from the same source as the primary antibody was applied. Formalin-fixed, paraffin-embedded sections from an invasive uterine cervix squamous cell carcinoma biopsy served as a positive control for $p16^{INK4a}$.

Supplementary materials related to this article can be found online at doi: 10.1016/j.virol.2011.10.011.

## Acknowledgments

Assignment of the HPV type number was kindly performed by Ethel-Michele de Villers, Human Papillomavirus Reference Laboratory, DKFZ, Heidelberg, Germany. We would like to express our appreciation to Takashi Yugawa, Tomomi Nakahara, and Shin-ichi Ohno for helpful discussions.

## References

Bates, S., Phillips, A.C., Clark, P.A., Stott, F., Peters, G., Ludwig, R.L., Vousden, K.H., 1998. p14ARF links the tumour suppressors RB and p53. Nature 395, 124–125.
Bernard, H.U., Burk, R.D., Chen, Z., van Doorslaer, K., Hausen, H., de Villiers, E.M., 2010. Classification of papillomaviruses (PVs) based on 189 PV types and proposal of taxonomic amendments. Virology 401, 70–79.
de Villiers, E.M., Fauquet, C., Broker, T.R., Bernard, H.U., zur Hausen, H., 2004. Classification of papillomaviruses. Virology 324, 17–27.
Doorbar, J., Coneron, I., Gallimore, P.H., 1989. Sequence divergence yet conserved physical characteristics among the E4 proteins of cutaneous human papillomaviruses. Virology 172, 51–62.
Egawa, K., 1988. Another viral inclusion wart different from myrmecia. Nippon Hifuka Gakkai Zasshi 98, 1105–1112.
Egawa, K., 1994. New types of human papillomaviruses and intracytoplasmic inclusion bodies: a classification of inclusion warts according to clinical features, histology and associated HPV types. Br. J. Dermatol. 130, 158–166.
Egawa, K., 2005. Histochemical analysis of cutaneous HPV-associated lesions. Methods Mol. Med. 119, 27–40.
Egawa, K., 2007. Genus gamma- and mu-papillomaviruses: clinical and histopathological aspects suggestive of their important roles in virology and human pathology. Current Topics in Virology 6, 53–66.
Egawa, K., Delius, H., Matsukura, T., Kawashima, M., de Villiers, E.M., 1993. Two novel types of human papillomavirus, HPV 63 and HPV 65: comparisons of their clinical and histological features and DNA sequences to other HPV types. Virology 194, 789–799.
Forslund, O., Antonsson, A., Nordin, P., Stenquist, B., Hansson, B.G., 1999. A broad range of human papillomavirus types detected with a general PCR method suitable for analysis of cutaneous tumours and normal skin. J. Gen. Virol. 80 (Pt 9), 2437–2443.
Hiraiwa, A., Kiyono, T., Suzuki, S., Ohashi, M., Ishibashi, M., 1996. E7 proteins of four groups of human papillomaviruses, irrespective of their tissue tropism or cancer

association, possess the ability to transactivate transcriptional promoters E2F site dependently. Virus Genes 12, 27–35.
Honda, A., Iwasaki, T., Sata, T., Kawashima, M., Morishima, T., Matsukura, T., 1994. Human papillomavirus type 60-associated plantar wart. Ridged wart. Arch Dermatol 130, 1413–1417.
Jablonska, S., Orth, G., 1985. Epidermodysplasia verruciformis. Clin. Dermatol. 3, 83–96.
Jablonska, S., Orth, G., Obalek, S., Croissant, O., 1985. Cutaneous warts. Clinical, histologic, and virologic correlations. Clin. Dermatol. 3, 71–82.
Kawai, K., Egawa, N., Kiyono, T., Kanekura, T., 2009. Epidermodysplasia-verruciformis-like eruption associated with gamma-papillomavirus infection in a patient with adult T-cell leukemia. Dermatology 219, 274–278.
Li, L., Barry, P., Yeh, E., Glaser, C., Schnurr, D., Delwart, E., 2009. Identification of a novel human gammapapillomavirus species. J. Gen. Virol. 90, 2413–2417.
Lutzner, M.A., Orth, G., Dutronquay, V., Ducasse, M.F., Kreis, H., Crosnier, J., 1983. Detection of human papillomavirus type 5 DNA in skin cancers of an immunosuppressed renal allograft recipient. Lancet 2, 422–424.
Nam, E.J., Kim, J.W., Hong, J.W., Jang, H.S., Lee, S.Y., Jang, S.Y., Lee, D.W., Kim, S.W., Kim, J.H., Kim, Y.T., Kim, S., 2008. Expression of the p16 and Ki-67 in relation to the grade of cervical intraepithelial neoplasia and high-risk human papillomavirus infection. J Gynecol Oncol 19, 162–168.
Queiroz, C., Silva, T.C., Alves, V.A., Villa, L.L., Costa, M.C., Travassos, A.G., Filho, J.B., Studart, E., Cheto, T., de Freitas, L.A., 2006. Comparative study of the expression of cellular cycle proteins in cervical intraepithelial lesions. Pathol. Res. Pract. 202, 731–737.
Schmitt, A., Harry, J.B., Rapp, B., Wettstein, F.O., Iftner, T., 1994. Comparison of the properties of the E6 and E7 genes of low- and high-risk cutaneous papillomaviruses reveals strongly transforming and high Rb-binding activity for the E7 protein of the low-risk human papillomavirus type 1. J. Virol. 68, 7051–7059.
Tamura, K., Dudley, J., Nei, M., Kumar, S., 2007. MEGA4: Molecular Evolutionary Genetics Analysis (MEGA) software version 4.0. Mol. Biol. Evol. 24, 1596–1599.
Thompson, J.D., Higgins, D.G., Gibson, T.J., 1994. CLUSTAL W: improving the sensitivity of progressive multiple sequence alignment through sequence weighting, position-specific gap penalties and weight matrix choice. Nucleic Acids Res. 22, 4673–4680.

JVI
Journals.ASM.org

# The E1 Protein of Human Papillomavirus Type 16 Is Dispensable for Maintenance Replication of the Viral Genome

**Nagayasu Egawa,[a] Tomomi Nakahara,[a] Shin-ichi Ohno,[a] Mako Narisawa-Saito,[a] Takashi Yugawa,[a] Masatoshi Fujita,[a,b] Kenji Yamato,[c] Yukikazu Natori,[d] and Tohru Kiyono[a]**

Division of Virology, National Cancer Center Research Institute, Tsukiji, Chuo-ku, Tokyo, Japan[a]; Department of Cellular Biochemistry, Graduate School of Pharmaceutical Sciences, Kyushu University, Maidashi, Higashi-ku, Fukuoka, Japan[b]; Section of Bacterial Pathogenesis, Tokyo Medical and Dental University, Graduate School of Medical and Dental Science, Yushima, Bunkyo-ku, Tokyo, Japan[c]; and RNAi Company Ltd., Hongo, Bunkyo-ku, Tokyo, Japan[d]

**Papillomavirus genomes are thought to be amplified to about 100 copies per cell soon after infection, maintained constant at this level in basal cells, and amplified for viral production upon keratinocyte differentiation. To determine the requirement for E1 in viral DNA replication at different stages, an E1-defective mutant of the human papillomavirus 16 (HPV16) genome featuring a translation termination mutation in the E1 gene was used. The ability of the mutant HPV16 genome to replicate as nuclear episomes was monitored with or without exogenous expression of E1. Unlike the wild-type genome, the E1-defective HPV16 genome became established in human keratinocytes only as episomes in the presence of exogenous E1 expression. Once established, it could replicate with the same efficiency as the wild-type genome, even after the exogenous E1 was removed. However, upon calcium-induced keratinocyte differentiation, once again amplification was dependent on exogenous E1. These results demonstrate that the E1 protein is dispensable for maintenance replication but not for initial and productive replication of HPV16.**

Papillomaviruses (PVs) are small, double-stranded DNA viruses that infect stratified squamous epithelium. Human PVs (HPVs) are very important causative agents for various lesions, ranging from verrucas to cancer. Among them, a subset of HPVs, the so-called high-risk types such as type 16 and 18, are associated with more than 90% of all cervical carcinomas as primary etiological factors (45). PVs establish long-term persistent infections in squamous epithelium, and the viral life cycle is tightly linked with the differentiation state of the host keratinocytes (7).

PV genome is replicated and amplified in three different stages: establishment, maintenance, and productive stages of the life cycle. In the establishment stage, soon after infection of the basal layer keratinocytes, a single or a few initial copies of the viral genome amplify and establish residence as multicopy circular extrachromosomal elements (episomes) in the nucleus. In the maintenance stage, the viral genomes in each affected cell replicate approximately once in a cell cycle in proliferating basal layer keratinocytes. Then, in the productive stage, they are exponentially amplified in terminally differentiating keratinocytes and packaged into progeny virions. It is important to understand the molecular mechanisms underlying this triphasic model for development of new therapies against HPV-infected lesions, such as cervical intraepithelial neoplasias, which can progress to cervical cancer.

The regulation of viral DNA replication is thought to differ in these three distinct stages of the viral life cycle. Studies of lesions experimentally induced by rabbit oral papillomavirus (ROPV) infection showed that the genome copy number of ROPV is low in the basal layer and increases up to four orders of magnitude during the terminal differentiation of host keratinocytes (21). This corresponds to more than 13 rounds of continuous replication of the viral genome in the productive stage.

Most of our knowledge of PV replication is derived from short-term replication assays to identify the components required for replication of the viral genome. These transient replication assays suggest that both viral proteins E1, a DNA helicase, and E2, a transcriptional activator and auxiliary replication factor, as well as *cis*-acting elements, including the E1-binding site (E1BS), several E2-binding sites (E2BS), and an AT-rich region in the long control region (LCR), are all essential for efficient PV DNA replication (4, 6, 20, 23, 30, 35, 37, 38). These studies appear to have analyzed the molecular mechanisms of viral replication in the productive stage, though they did not necessarily examine the three stages separately.

In this context, it is of interest that the HPV genome lacking LCR can replicate in the absence of both E1 and E2 proteins in transient replication assays (1, 16, 29), and a temperature-sensitive (TS) E1 mutant of bovine papillomavirus type 1 (BPV1) can be maintained in mouse C127 cells at a nonpermissive temperature as efficiently as the wild-type BPV1 (17). These reports suggest that E1 might be dispensable for maintenance replication.

To test this hypothesis directly, we here used an E1-defective mutant HPV16 genome featuring a translation termination mutation in E1. We established human dermal keratinocytes (HDKs) containing the E1-defective HPV16 genome with the help of exogenous E1 expression and then removed the exogenous E1 expression cassette with the FLP/FRT system (36). Similar to the wild-type genome, the E1-defective HPV16 genome was maintained for numerous cell generations without exogenous E1 expression. However, unlike the wild-type genomes, the E1-defective HPV16 genome failed to amplify upon differentiation of host cells, with rescue dependent on reexpression of exogenous E1. These results indicate that HPV16 requires E1 protein for the

**Received** 1 October 2011 **Accepted** 3 January 2012
**Published ahead of print** 11 January 2012
Address correspondence to Tohru Kiyono, tkiyono@ncc.go.jp

doi:10.1128/JVI.06450-11

TABLE 1 Primers for PCR and RT-PCR

| Name | nt position | Sequence (5′→3′) | Product size |
|---|---|---|---|
| For detecting excision of HPV16 DNA[a] | | | |
| For total HPV DNA, HPV16 E7 | 660 | GGAGGAGGATGAAATAGATGGTC | 136 |
| | 795 | AGTACGAATGTCTACGTGTGTGC | |
| For excised-circular HPV DNA, HPV16 LCR | 7432 | AGGCCCATTTTGTAGCTTC | 271 |
| | 7702 | CCTAACAGCGGTATGTAAGG (+loxP 305) | |
| For detecting mRNAs | | | |
| HA-E1 | 7 | CCTTATGACGTGCCAGATTACGC | 144 |
| | 150 | GTCATTTTCGTTCTCATCGTCTGAGATG | |
| E1^E4 | 603 | TTTGCAACCAGAGACAACTGAT | 933 |
| | 4014 | AGAGGCTGCTGTTATCCACAAT | |
| 36B4[b] | 655 | TCGACAATGGCAGCATCTAC | 223 |
| | 877 | GCCTTGACCTTTTCAGCAAG | |
| For real-time quantitative PCR to quantify HPV16 DNA | | | |
| HPV16 L2 | 4474 | CCCACAGCTACAGATACACTTGCT | 143 |
| | 4616 | GGAATGGAAGGTACAGATGTTGGTGC | |

[a] GenBank accession number for HPV16 is K02718.
[b] GenBank accession number for 36B4 is M17885.

establishment and the productive stages but not for the maintenance stage of viral genome replication. The results have important implications for the development of E1 inhibitors as anti-HPV drugs.

## MATERIALS AND METHODS

**Cell culture.** Human dermal keratinocytes (HDKs) were purchased from Cell Applications (San Diego, CA). HDKs were immortalized with TERT, a mutant form of CDK4 and cyclin D1 (HDK-K4DT) by lentivirus-mediated gene transfer as described below. The cells were maintained in low-calcium serum-free keratinocyte growth medium (Epilife, Invitrogen, Carlsbad, CA) unless otherwise described. To induce keratinocyte differentiation, cells were exposed to Epilife basal medium supplemented with 1.8 mM $CaCl_2$ for 7 days or more. W12 (20863) cells were obtained from Paul F. Lambert (McArdle Laboratory for Cancer Research, Madison, WI) and cultured on mitomycin-treated Swiss mouse 3T3 cells in F medium as previously described (13).

**Plasmid construction.** In pCMV-loxP-HPV16-loxP-puro, the full-length HPV16 genome linearized at the SphI site in the long control region and flanked by *loxP* recombination sites (18) was inserted between a CMV promoter and a puromycin resistance gene so that the HPV16 genome was located in reverse orientation to the CMV promoter to avoid CMV-driven expression of HPV16 genes. In pCMV-loxP-E1-defective HPV16-loxP-puro, an in-frame stop codon was created at nucleotides (nt) 892 to 894 just downstream of the E1 start codon at nucleotide 865 by site-directed mutagenesis. The segment encoding Cre recombinase with nuclear localization signal in AxCANCre (14) was cloned into pcDNA3 (Invitrogen) to generate pcDNA3-NCre. Detailed methods for the construction of pCMV-loxP-HPV16-loxP-puro, pCMV-loxP-E1-defective-HPV16-loxP-puro, and pcDNA3-NCre are available upon request.

**DNA transfection.** HDK-K4DT cells were seeded at a density of $2 \times 10^5$ cells onto six-well plates (BD Biosciences, Franklin Lakes, NJ) containing 2 ml of Epilife and incubated overnight and then cotransfected with 1 $\mu$g of pcDNA3-NCre and 3 $\mu$g of pCMV-loxP-HPV16-loxP-puro (wild-type or E1-defective strains) using FuGENE HD (Roche). One day after transfection, cells were selected by 1 $\mu$g/ml of puromycin for 2 days.

**Vector construction and retroviral infection.** Construction of lentiviral vectors, CSII-CMV-TERT, CSII-CMV-cyclin D1, and CSII-CMV-$CDK4^{R24C}$, were described previously (33). CSII-CMV-TetON-ADV contains the TetON-ADV segment from pTet-On Advanced Vector (Clontech, Mountain View, CA). To yield improved E1 gene expression in mammalian cells, the codon-optimized HPV16 E1 gene with an N-terminal hemagglutinin (HA) tag (HA16E1) was synthesized (GenScript, Piscataway, NJ). CSII-TRE-Tight-HA16E1 contains the HA16E1 gene under the control of the tetracycline responsive promoter from pTRE-Tight (Clonetech). pCMSCV-FRT-HA-E1-TKneo consists of the CMV/LTR fusion promoter, the $\Psi$ packaging signal, a mutant (f72) FLP recognition target (5′FRT) (24), the HA16E1 gene, the PKG promoter, and the herpes simplex virus thymidine kinase (HSV-TK) fused to the neomycin-resistant gene (*neo*), 3′FRT, and 3′LTR, as shown in Fig. 3A. Cells infected with this retrovirus were positively or negatively selected in the presence of 50 $\mu$g/ml of G418 or 10 $\mu$g/ml of ganciclovir, respectively. The nucleotide sequence of the HA16E1 and the detailed methods for the construction of pCMSCV-FRT-HA16E1-TKneo-FRT, CSII-CMV-TetON-ADV, and CSII-TRE-Tight-HA16E1 are available upon request. The production of recombinant retroviruses and lentiviruses was accomplished as described previously (27, 33).

**AdV.** The thermostable FLP mutant (FLPe)-expressing adenovirus vector (AdV) (AxCAFLPe), a kind gift from Izumi Saito (The Institute of Medical Science, The University of Tokyo), was prepared as described previously (3, 36). Cells were infected with AxCAFLPe at a 5-particle titer multiplicity of infection.

**Western analysis.** Western blotting was conducted as described previously (26). Antibodies against HA (16B12; Covance, Princeton, NJ), involucrin (SY5; Sigma-Aldrich, St. Louis, MO), vinculin (Sigma-Aldrich), and loricrin (Covance) were used as probes, and horseradish peroxidase-conjugated anti-mouse, anti-rabbit (Jackson ImmunoResearch Laboratories, West Grove, PA), or anti-goat (sc-2033; Santa Cruz, Santa Cruz, CA) immunoglobulins were employed as secondary antibodies.

**PCR and DNA blot hybridization.** Total genomic DNA was isolated by a standard SDS-proteinase K method, and an aliquot (100 ng) was examined by PCR amplification for Cre-mediated HPV DNA excision. Primer sets used for detecting total HPV16 DNA or recombined HPV16 are shown in Table 1. The DNA was amplified by 30 cycles of PCR using Takara *Taq* DNA polymerase (Takara, Japan) according to the supplier's instructions, with annealing at 60°C and elongation at 72°C for 30 s. PCR products were separated on a 1.5% agarose gel and visualized with ethidium bromide. For Southern blot analyses, digested DNA was separated on a 0.75% agarose gel, soaked in 0.25 M HCl for 15 min, and alkaline transferred onto nylon membranes (Boehringer Mannheim, Mannheim, Germany). The membranes were prehybridized in Hybrisol I

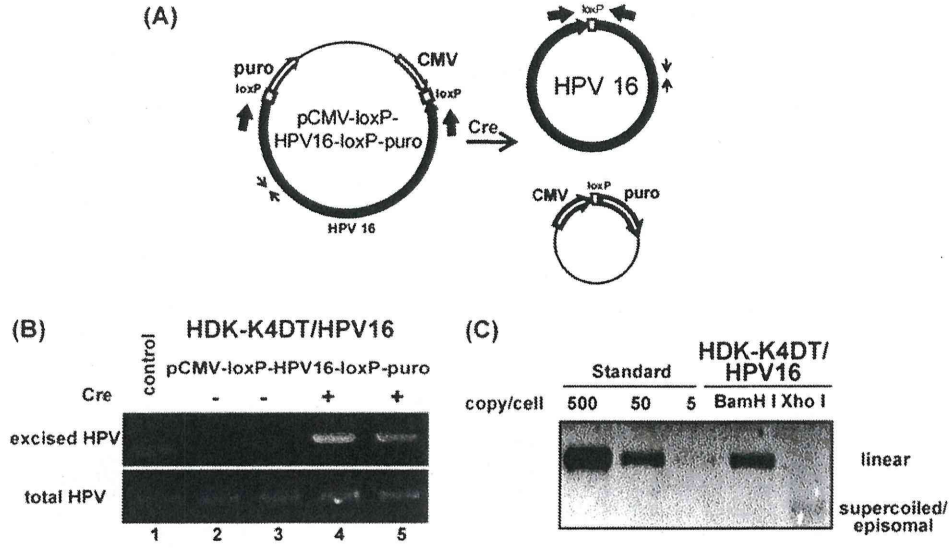


FIG 1 HPV genome excision and establishment of the cell line containing the HPV16 genome. (A) Schematic representation describing the parental pCMV-loxP-HPV16-loxP-puro, the Cre recombinase-excised HPV16 genome, and the pCMV-puro plasmid. PCR primers (thin and thick arrows) to detect total and excised HPV DNA, respectively, are indicated. (B) HDK-K4DT cells were cotransfected with the pCMV-loxP-HPV16-loxP-puro plasmid with (lanes 4 and 5) or without (lanes 2 and 3) the NCre expression plasmid. Total DNA was extracted from the cells 2 days after the transfection without puromycin selection. Representative pictures of an ethidium bromide-stained agarose gel with PCR products indicating total HPV16 DNA (bottom) and excised circular HPV16 DNA (top), containing a surplus of 34 bp of *loxP* DNA, are shown. (C) Southern blot hybridization for the HPV genome in HDK-K4DT cultures. DpnI and BamHI- or XhoI-digested total DNA isolated from HDK-K4DT at 3 weeks after transfection with pCMV-loxP-HPV16-loxP-puro plasmid and the NCre expression plasmid is shown. Digestion with BamHI, which cuts the HPV16 genome once, produced results of the expected size for the HPV16 genome. Digestion with XhoI, which does not cut the HPV16 genome, showed supercoiled plasmid of HPV16 genome. The BamHI-linearized HPV16 plasmid was used for length and copy number standards.

(Millipore, Billerica, MA) for 1 h at 42°C. A biotin-labeled probe of the entire HPV16 genome prepared with the NEBlot Phototope kit (New England BioLabs, Ipswich, MA) was applied for hybridization, and the hybridized DNA was visualized with a Phototope-Star detection kit (New England BioLabs) following the protocol provided by the manufacturer. The LAS3000 charge-coupled device (CCD) imaging system (Fujifilm Co. Ltd., Japan) was employed for detection and quantification.

**RNA extraction and RT-PCR analyses.** For detection of mRNAs, total RNA was purified with RNeasy (Qiagen, Valencia, CA) and reverse transcribed to generate cDNAs by the ThermoScript reverse transcription (RT)-PCR system (Invitrogen) using random hexamers according to the supplier's instructions. Primers used for the E1^E4 spliced transcript, exogenous codon optimized E1, and human acidic ribosomal phosphoprotein P0 (36B4) are shown in Table 1. The thermocycling profile for amplifying E1^E4, E1, and 36B4 cDNAs was 1 min at 95°C; 40 cycles of 95°C for 30 s, 54°C for 30 s, and 72°C for 30 s (or 1 min for E1^E4 cDNA); and 4 min of extension at 72°C. PCR products were separated in a 1.5 or 0.9% agarose gel and visualized with ethidium bromide.

**Quantitative real-time PCR for genomic DNA.** Reactions were prepared in a volume of 10 μl containing 1× quantitative PCR (qPCR) master mix of KAPA SYBR FAST qPCR kits (Kapa Biosystems, Woburn, MA) and 300 nM each primer. PCR was performed using StepOnePlus (Applied Biosystems) with 10 s of denaturation at 95°C followed by 40 cycles of 95°C for 3 s and 60°C for 30 s. Serial dilutions of linearized HPV16 genome from pUC-HPV16 plasmid DNA by BamHI digestion were used as controls to measure the amounts of HPV16 genomic DNA. All real-time PCRs were run in triplicate. Total DNA was digested with DpnI before PCR amplification of the HPV16 genome with a primer set amplifying a product containing two DpnI sites (Table 1). HPV16 DNA copy number was expressed as copies per cell assuming that the total human genomic DNA is 6.6 pg/diploid cell. The rate of HPV16 genome retention (RR) was calculated as follows: RR = (copy number of viral genomes at the end/copy number of viral genomes at the beginning) 1/PD, where population doubling (PD) of cells was calculated as follows: PD = log(number of cells obtained/initial number of cells)/log2.

## RESULTS

**Establishment of keratinocytes containing the HPV16 genome.** Primary human keratinocytes are often used for establishment of HPV-containing cell lines. However, they have a finite life span, and cells harboring HPV genomes tend to preferentially grow in culture. To minimize this effect and to obtain reproducible results, we first immortalized human dermal keratinocytes (HDKs) with TERT, a mutant form of CDK4 and cyclin D1 (HDK-K4DT). HDK-K4DT formed fully stratified squamous epithelium in an organotypic raft culture (data not shown). Then, we established keratinocytes harboring HPV genomes as episomes. HDK-K4DT cells were transfected with pCMV-loxP-HPV16-loxP-puro, designed to generate a circular 7.9-Kb HPV16 genome and a circular pCMV-puro expression cassette (Fig. 1A). With the Cre expression plasmid, about 5 to 10% of the transfected cells survived after short-term puromycin selection, whereas only a few cells survived without Cre recombinase (data not shown). At 2 days posttransfection without puromycin selection, total DNA was analyzed by PCR using two sets of primers, one for total HPV16 DNA and the other specific for the circularized HPV16 genome (Fig. 1A). In cells cotransfected with Cre, PCR products corresponding to the recombined circular HPV16, whose size should be bigger by 34 bp due to an inserted *loxP* sequence, were observed (Fig. 1B, lanes 4 and 5), whereas no circularized HPV16 genome was detected in cells without Cre expression (Fig. 1B, lanes 2 and 3). Southern blot analysis of total DNA extracted from cells at 21 days posttransfection suggested that the established HDK-K4DT cells harbored

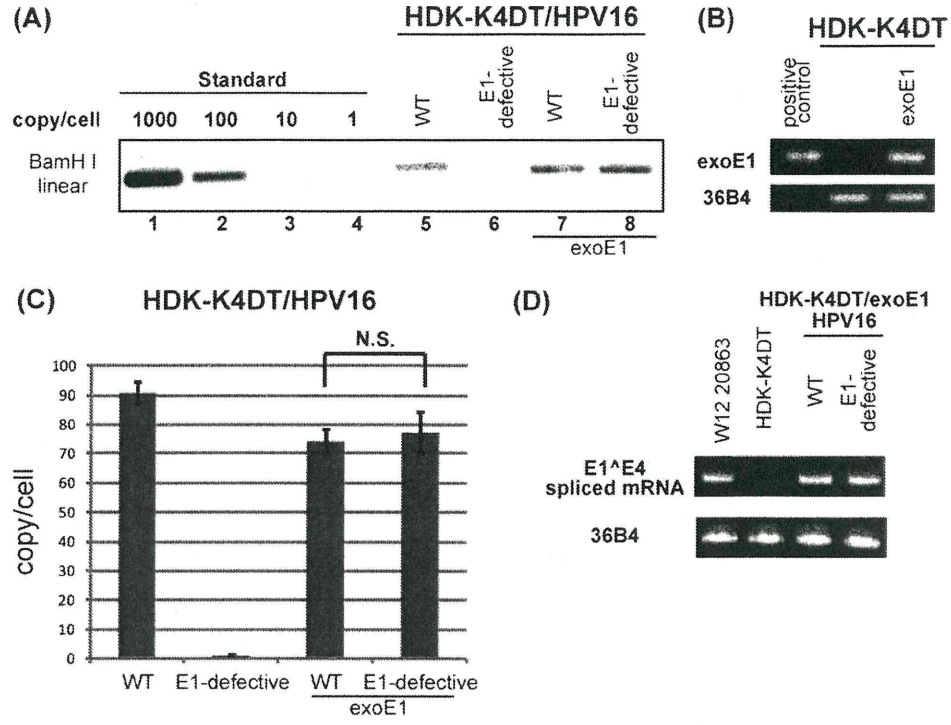


FIG 2 Requirement for E1 protein in the establishment stage. (A) Southern blot hybridization of the HPV genome in HDK-K4DT cultures. Parental (lanes 5 and 6) and exogenous E1 expressing HDK-K4DT cells (lanes 7 and 8) were transfected with the wild-type (WT) or the E1-defective pCMV-loxP-HPV16-loxP-puro plasmid and the NCre expression plasmid. Total DNA was extracted at 21 days posttransfection. DpnI- and BamHI-digested total DNA from parental or exogenous E1 expressing HDK-K4DT cultures was analyzed. The BamHI-linearized HPV16 plasmid was used for length and copy number standards (lanes 1 to 4). (B) mRNAs for exogenous E1 of HDK1-K4DT cells transduced with the retroviral vector expressing HA16E1 were analyzed. Total RNAs isolated from cells with or without the retroviral transduction were subjected to reverse transcription (RT)-PCR with a primer set specific to codon-optimized E1. 36B4 mRNA was also detected as an internal control. The PCR products of exogenous E1 (top) and 36B4 (bottom) visualized in ethidium bromide-stained agarose gels are shown. pCMSCV-FRT-HA16E1-TKneo-FRT was used as a positive control. (C) The copy number of the HPV16 genomes at 14 days posttransfection in each HDK-K4DT cell lines was determined by real-time PCR. The deviations of three independent sets of transfectants are shown as error bars. N.S., not significant. (D) Expression of the E1^E4 spliced mRNAs in E1-expressing HDK-K4DT cells harboring the wild type or the E1-defective HPV16 genomes at 35 days posttransfection. Total RNAs were subjected to RT-PCR with an E1^E4-specific primer set (Table 1). RNAs from parental HDK-K4DT cells and W12 cells were used as controls. PCR products of E1^E4 (top) and 36B4 (bottom) are shown, as described for panel B.

more than 50 viral genome copies per cell (Fig. 1C). Repeated transfection experiments confirmed the reproducibility of this technique. At 60 days posttransfection, after nine serial passages at a ratio of 1:8, we still detected 10 to 20 copies of the viral genomes per cell (data not shown). The rate of HPV16 genome retention was calculated as 90% per cell division.

**E1 protein is required for establishment of HPV16 genomes as episomes in HDK-K4DT cells.** To study the role of E1 in each stage of the viral life cycle, we prepared an E1-defective mutant HPV16 genome containing an E1 translation termination mutation at nt 892 to 894 to abrogate E1 protein expression. Unlike the wild-type HPV16 genome, the HPV16 E1-defective genome failed to establish in HDK-K4DT cells as episomes (Fig. 2A, lanes 5 and 6). However, in HDK-K4DT cells expressing exogenous E1 from the retrovirus, MSCV-FRT-HA16E1-TKneo-FRT, the E1-defective HPV16 genome could establish as episomes as efficiently as the wild type HPV16 genome (Fig. 2A, lanes 7 and 8). We confirmed the expression of exogenous E1 driven by the LTR promoter by RT-PCR using primers specific for exogenous E1 (Fig. 2B), though the E1 protein was undetectable by Western blot analysis. The copy numbers of the E1-defective HPV16 genome were comparable to that of the wild-type HPV16 genome in the presence of exogenous E1 expression (Fig. 2C). The translation termination mutation inserted in the downstream of the splice donor site for E1^E4 (nt 880) did not disrupt normal E1^E4 splicing (Fig. 2D). These data indicate that the E1 protein is required for initial replication and/or maintenance of the viral genome.

**E1 protein is dispensable for maintenance replication of the viral genome.** In order to assess the requirement of E1 protein for maintenance replication of the viral genome, we used the HDK-K4DT cells harboring the E1-defective HPV16 genomes established with exogenous E1 expression from the integrated MSCV-FRT-HA16E1-TKneo-FRT retrovirus. Upon infection of FLPe-expressing AdV, the exogenous E1 expression cassette as well as the TKneo gene was excised by FLP at an efficiency of around 50% (Fig. 3A). Then we isolated HDK-K4DT cells which no longer expressed exogenous E1 by ganciclovir selection (Fig. 3B). After several passages of cells at a ratio of 1:8, the copy number of HPV16 genomes was determined by real-time PCR. We detected 70 to 100 copies of the wild-type or the E1-defective HPV16 genomes per cell just before the AdV infection. Copy numbers of both the wild-type and the E1-defective HPV16 genomes gradually decreased during the passages (Fig. 3C). However, about 10 to 20 copies of the E1-defective HPV16 genomes

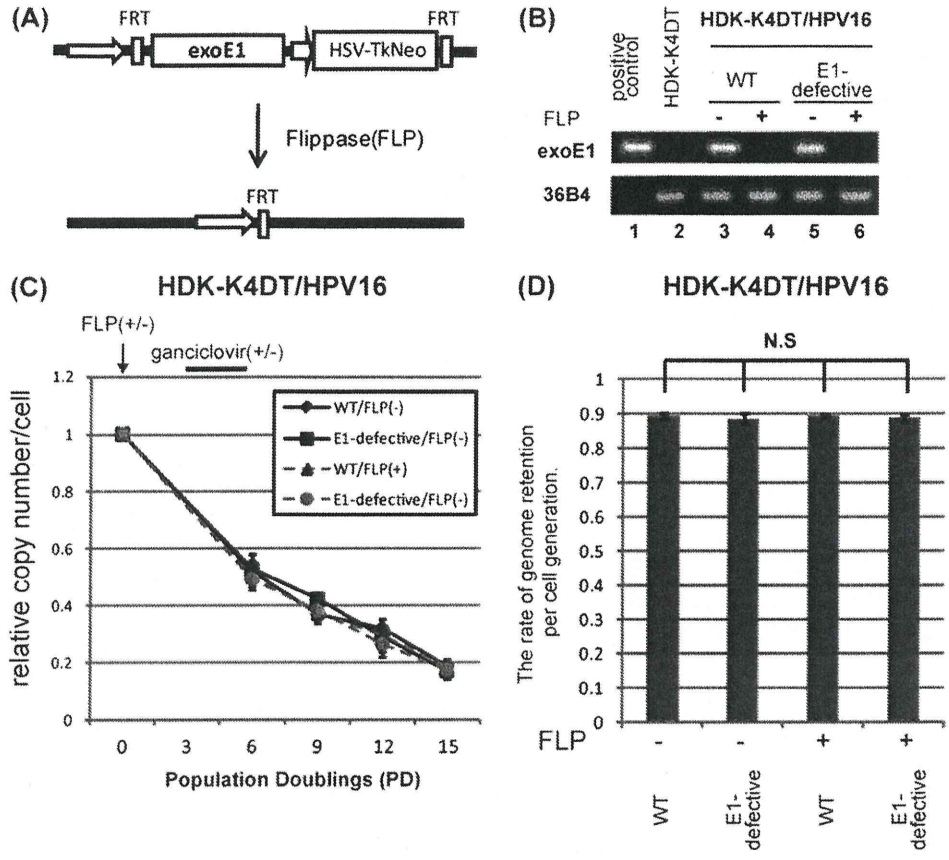


FIG 3 E1 protein is not essential for maintenance replication of the viral genome. (A) Schematic representation of the viral vector, MSCV-FRT-HA16E1-TKneo-FRT, expressing exogenous E1. The HA-tagged HPV16 E1 gene and the TKneo fusion gene are flanked by FLP recognition target (FRT) sites. When a thermostable FLP-expressing AdV (AxCAFLPe) is infected, the DNA in between the FRT sites is excised so that exogenous E1 as well as TKneo expression is terminated. Cells still expressing E1 and HSV-TK can be negatively selected with ganciclovir. (B) mRNAs containing exogenous E1 message were analyzed to ensure complete removal of E1 expression. Total RNAs isolated from HDK-K4DT/HPV16 cell lines at 21 days postinfection with (lanes 4 and 6) or without (lanes 3 and 5) AxCAFLPe were subjected to RT-PCR with a primer set specific to codon-optimized E1. Representative pictures of an ethidium bromide-stained agarose gel with PCR products indicating exogenous E1 (top) and 36B4 (an internal control; bottom) are shown. pCMSCV-FRT-HA16E1-TKneo-FRT was used as a positive control. (C) HDK-K4DT cells containing the wild type (WT) or the E1-defective HPV16 genome were established in the presence of exogenous E1 expression. Two weeks after transfection, aliquots of cells were infected with AxCAFLPe (FLP +) at a multiplicity of infection of 5, followed by selection with 10 $\mu$g/ml of ganciclovir for 1 week. After the selection, cells were cultured for 4 passages at a ratio of 1:8 to examine the retention rate of the wild-type or the E1-defective genome in the presence or the absence of exogenous E1. HDK-K4DT/HPV16 cells which were not infected with AxCAFLPe (FLP−) were also cultured for 5 passages at a ratio of 1:8. Total DNA was extracted just before the infection, at every passage and at the end of the culture. The copy number of HPV16 genomes was measured by real-time PCR and normalized to the total amount of DNA. The graph shows time courses of copy number change during the 5 passages after the infection. The copy number at the each time point is shown as a ratio to the copy number just before the FLP-expressing adenovirus infection (PD0). The end of the ganciclovir selection corresponds to PD6. Means and standard errors of the means are shown. (D) The graph shows the rates of HPV genome retention per cell division. The retention rates were calculated as described in Materials and Methods. Means from three independent experiments and standard deviations are shown as error bars. N.S., not significant, compared with each other.

per cell still remained after several passages of cells, even in the absence of exogenous E1 expression. No difference in the rate of genome retention was observed between the E1-defective and the wild-type HPV16 genomes. The rates were calculated as approximately 90% per cell division, irrespective of exogenous E1 expression, and proved quite constant in three independent experiments (Fig. 3D). These data indicate that the E1 protein is dispensable for maintenance replication of the viral genome.

**E1 protein is required for viral genome amplification upon differentiation.** To confirm that E1 protein is required for the productive stage of viral replication, differentiation-dependent viral genome amplification was examined with the same series of the cells established for the previous section (Fig. 3). HDK-K4DT cells harboring the wild-type or the E1-defective HPV16 genomes in the presence or the absence of exogenous E1 expression were exposed to a high calcium concentration. Induction of differentiation was confirmed by expression of keratinocyte differentiation markers, involucrin and loricrin (Fig. 4A). Southern blot analyses of DNA extracted from sister cultures showed the wild-type HPV16 genomes to be amplified episomally upon differentiation in the absence of exogenous E1 expression (Fig. 4B, lanes 1 to 2). However, the E1-defective HPV16 genomes were amplified only in the presence of exogenous E1 expression (Fig. 4B, lanes 3 to 6). Reintroduction of E1 with lentiviruses, CSII-CMV-tetON and CSII-TRE-Tight-HA16E1, to the cells whose exogenous E1 cassette had been excised by FLP rescued the E1-defective HPV16 genome amplification upon differentiation only when the E1 expression was induced by doxycycline (Fig. 4B, lanes 7 and 8),

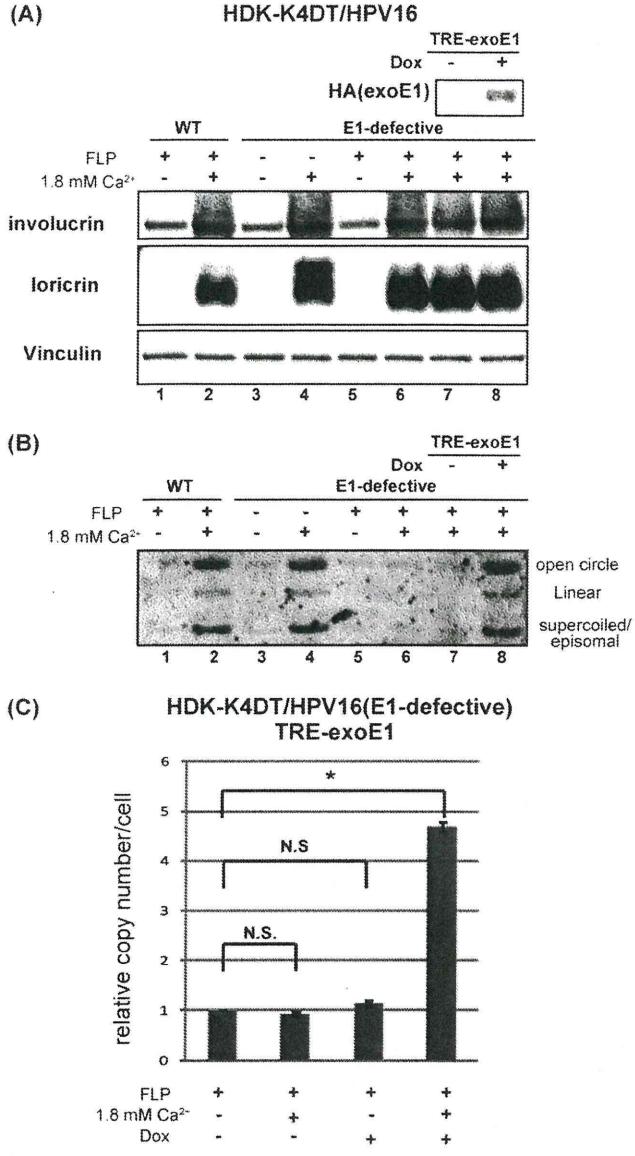


FIG 4 E1 protein is required for viral genome amplification upon differentiation. (A) HDK-K4DT cells harboring the wild-type (lanes 1 and 2) or the E1-defective (lanes 3 to 8) HPV16 genomes in the presence (FLP−, lanes 3 and 4) or the absence (FLP+, lanes 1 and 2, 5 to 8) of exogenous E1 expression were seeded at $2 \times 10^5$ cells per well (6-well plate) in Epilife complete growth medium, and then cells were exposed to 1.8 mM calcium (lanes 2, 4, 6, 7, 8) to induce keratinocyte differentiation. Total cell lysates were made, and total DNAs were extracted from the sister cultures just before and 10 days after calcium exposure. The expression of involucrin and loricrin, keratinocyte differentiation markers, was analyzed by Western blotting. Expression of reintroduced exogenous E1 controlled by doxycycline was detected by anti-HA antibody (lanes 7 and 8). Vinculin was detected as a loading control. (B) Southern blot hybridization for episomal HPV16 genomes in HDK-K4DT cells. XhoI-digested total DNA from each HDK-K4DT culture was loaded. A representative image of three independent experiments is shown. (C) The copy number of the E1-defective HPV16 genomes in HDK-K4DT cells in the indicated condition was determined by real-time PCR. Three replicates are shown and standard deviations are shown as error bars. N.S., not significant. The single asterisk indicates $P$ values of $<0.05$.

whereas induction of E1 alone without high calcium failed to rescue the genome amplification (Fig. 4C). These data indicate that E1 protein is required for viral genome amplification upon differentiation. Since the same series of cells used for Fig. 3 were used in these experiments, the results confirmed that the E1-defective HPV16 genomes were episomally maintained in the absence of E1 expression.

## DISCUSSION

In this study, we demonstrated that E1 is dispensable for maintenance replication of the HPV16 genome but required for replication in the establishment and productive stages. Taking the previous study using a TS E1 mutant of BPV1 (17) into account, it is likely that E1 is dispensable for the maintenance replication of other PVs, too.

Thus, HPVs have at least two replication modes and control the copy number of the viral genome depending on the situation. Such a strategy of the virus would clearly be beneficial for persistent infection and continuous virus production. In the maintenance phase, minimal expression of viral proteins in host cells with low copy numbers of viral genomes would allow HPV to evade cellular immune surveillance. Moreover, as recent studies indicate, a high level of E1 expression in basal-layer cells could activate an ATM-dependent damage response and cause growth suppression (10, 32).

It is reasonable to speculate that the E1-independent maintenance replication employs the cellular replication machinery to support viral genome maintenance under S phase control. Mechanisms of viral genome DNA replication control by host cell factors have been well studied for the Epstein-Barr virus (EBV). The EBV genome DNA is replicated once per S phase in the latent phase of infection (19, 44). In this phase, EBV employs replication licensing proteins, MCMs and ORC (19, 22), which assemble on the latent origin of replication of EBV, OriP. A low copy number for the viral genome may be an appropriate common strategy for episomal viruses to sustain latent infection. Although it is not known whether and how MCMs and ORC are involved in HPV DNA replication, E1- and E2-independent *cis*-replicating elements may reside outside the LCR and possibly in the late region (L2-L1 open reading frames [ORFs]) of the HPV16 genome (28, 29).

The observed rate of HPV16 genome retention was about 90% per cell generation, which is comparable to the reported rate for the EBV genome (25). With this retention rate, the viral genomes of 100 copies per cell can be maintained for 2 to 3 months, corresponding to approximately 40 cell divisions under our culture conditions. In the stratified squamous epithelium, stem cells self-renew by dividing infrequently and generate a population of cells that undergo limited but more frequent divisions before giving rise to nonproliferative, terminally differentiating cells. In the natural life cycle of HPVs, the virus must infect epithelial stem cells (8, 34), which would divide much less frequently than cultured cells do. Therefore, the viral genome in the stem cells *in vivo* would be able to persist for much longer period than in cultured cells, even if the genome retention rate is the same as that found in our study.

In maintenance replication, HPV may still employ two different modes of replication. Hoffmann et al. showed that HPV16 DNA replicates once per S phase in W12 cells, while HPV31 DNA replicates via a random-choice mechanism with some multiple